Response Inhibition in Healthy Subjects: Establishing and Examining an EEG Data Repository from Multiple Study Sites

Kevin D. **Prinsloo**[1], Edward G. **Freedman**[1], Pierfilippo De **Sanctis**[2], Kristen P. **Morie**[3,4], Kathryn-Mary **Wakim**[2], Eleni **Patelaki**[1], Douwe **Horthuis**[2], Ana A. **Francisco**[2], Sophie **Molholm**[2], and John J. **Foxe**[1,2]

[1] The Frederick J. and Marion A. Schindler Cognitive Neurophysiology Laboratory, The Del Monte Institute for Neuroscience, Department of Neuroscience, University of Rochester School of Medicine and Dentistry, Rochester, NY 14642, USA

[2] The Cognitive Neurophysiology Laboratory, Department of Pediatrics and Neuroscience, Albert Einstein College of Medicine, Bronx, New York, USA

[3] Department of Psychiatry, Yale University School of Medicine, New Haven, CT, 06510, USA Child Study Center

[4] Yale University School of Medicine, New Haven, CT, 06510, USA

Correspondence: John, Foxe: John J. Foxe PhD, Department of Biomedical Engineering, Department of Neuroscience, and Del Monte Institute for Neuroscience, University of Rochester, 201 Robert B. Goergen Hall, P.O. Box 270168, Rochester, NY 14627, USA.

John Foxe, John_Foxe@urmc.rochester.edu

Number of Figures: 9, Number of Tables: 6; Number of Multimedia: 0

Number of Words: Abstract – 293, Significance Statement – 69, Introduction – 2136, Discussion – 4523

Conflict of Interest: The authors declare no competing financial interests.

Acknowledgements: This work was supported by a []. The authors thank [ ] for assistance with data collection, and [ ] for helpful comments on this manuscript.

1 Abstract

The current paper introduces a combined human-participant high-density electroencephalography (EEG) recordings with behavior metrics from multiple sites using a set of similar response inhibition Go/NoGo tasks. The dataset consists of 302 healthy individuals (age range 7-92). Inhibitory control and performance monitoring are critical executive functions of the human brain. The current dataset offers a unique opportunity to leverage this large cohort to provide insight into normative neurobehavioral response inhibition and for novel exploration. In the current paper, we demonstrate the potential of the data repository, its efficacy and utility but replicating the main canonical findings in the literature including some novel findings. With increasing growth in Open Science with data sharing initiatives for neuroimaging studies, data repositories offer an opportunity to confront "*small N*" issues that blight current neuroimaging studies. Large datasets afford the opportunity to investigate underpowered experimental conditions and present opportunities to enhance reproducibility in neuroimaging research. To validate the efficacy of the provided data repository, the current paper replicates canonical response inhibition electrophysiological and behavioral components such as the classical N2 and P3 complex. Further, taking advantage of large quantity of trials it was possible to accurately characterize the event-related negativity associated with making inhibition errors and the typical slowing down of reaction time following error or conflict (post-error slowing). Using inter-trial phase coherence across the functional network the results showed a significant right hemisphere lateralized connectivity on both the theta and delta frequency ranges that were strongest at later latencies for Cr (NoGo) trials. The current data offer a unique opportunity to further explore the effects these subtle paradigm differences can have on electrophysiological and behavioral outcomes. The normative databases are useful tools for assessing deviations from the expected population parameters that may indicate markers of disease or degeneration.

2 Significance Statement

Over the past two decades, the call for open science has encouraged researchers to make available public data repositories of neuroimaging datasets from normative populations. The current paper introduces a data repository of 302 healthy controls performing small variants of a response inhibition task and presents findings that offer insights into the efficacy of the dataset. The repository offers a unique opportunity for replication and novel investigation for researchers.

3 Key words

Response inhibition (RI), inhibitory control, data repository, Open Science, EEG, collaborative research, data integration, neuroimaging, aging, event-related potentials (ERPs), N2, P3, event-related negativity (ERN), event-related positivity (Pe), Post-error slowing (PES), Post-error action control; Inter-trial-phase coherence (ITPC), BIDS

4 Introduction

Data sharing is one of the core tenets of open science. It is one of the main avenues to improve research reliability and reproducibility, data reuse and data integration. This manuscript presents a data repository that includes high-density electroencephalography (EEG), and measures of behavioral performance from 302 healthy controls performing a Go/NoGo response inhibition task. Small variations in task design and age differences in participants serve to provide additional insight into the mechanisms and development of response inhibition in a large healthy cohort.

Response inhibition and interference control form two hallmark features at the core of executive control and play a crucial role in generating flexible, goal-directed behavior in everyday life. Dysfunction in these mechanisms is considered integral to numerous neurological and psychiatric disorders, and more generally to a wide range of health and behavioral problems (Aron & Poldrack, 2005; Chamberlain, Fineberg, Blackwell, Robbins, & Sahakian, 2006; Francisco, Horsthuis, Popiel, Foxe, & Molholm, 2020; Groman, James, & Jentsch, 2009; Jentsch & Taylor, 1999; Krakowski et al., 2016; Morie, De Sanctis, Garavan, & Foxe, 2014; Roche et al., 2004; Wakim et al., 2021). Data presented here were collected across two sites: The Cognitive Neurophysiology Lab at the University of Rochester Medical Center (UoR) and The Cognitive Neurophysiology Lab at the Albert Einstein College of Medicine (EinMed). In compiling the data, only EEG recordings from healthy subjects were chosen and data consist of both published and unpublished work from each site (De Sanctis, Butler, Malcolm, & Foxe, 2014; De Sanctis et al., 2020; Francisco et al., 2020; Krakowski et al., 2016; Malcolm, Foxe, Butler, & De Sanctis, 2015; Malcolm et al., 2019; Morie, Garavan, et al., 2014; Patelaki, Foxe, Mazurek, & Freedman, 2022; Wakim et al., 2021). These data provide the opportunity to make comparisons of the standard Go/NoGo tasks and leverage the large cohort to provide some insight and replication of the main reported findings in the literature. This demonstrates the potential of the data repository, its efficacy and utility. Sharing provides the opportunity for independent replication of already published results from this dataset and novel exploration. The normative databases are useful tools for assessing deviations from the expected population parameters that may indicate markers of disease or degeneration.

Response inhibition paradigms have been used in neuroscience and clinical psychology to investigate underlying behavioral and neural mechanisms (Corbett & Constantine, 2006; Hester, Foxe, Molholm, Shpaner, & Garavan, 2005; Huster, Enriquez-Geppert, Lavallee, Falkenstein, & Herrmann, 2013; Riccio, Reynolds, Lowe, & Moore, 2002; Ruchsow et al., 2008; van Boxtel, van der Molen, Jennings, & Brunia, 2001). Specifically, response inhibition efficiency is correlated with

treatment outcome (Loree, Lundahl, & Ledgerwood, 2015; Van der Oord, Geurts, Prins, Emmelkamp, & Oosterlaan, 2012; Verbruggen et al., 2019; Verbruggen & Logan, 2008) in many clinical conditions. Go/NoGo or Stop Signal tasks have typically been used to assess response inhibition. Although these differ in some aspects, they are considered validated paradigms for measuring and assessing cognitive control of behavioral response inhibition, specifically motor inhibition (van Boxtel et al., 2001). Here the focus is on the Go/NoGo task (Konishi et al., 1999; Verbruggen & Logan, 2008). Despite its ubiquity and apparent simplicity, there are many features (ranging from task design to data analysis) that vary across studies which can ultimately affect the results and interpretations using this task.

Various studies have investigated the neural correlates of response inhibition (e.g. meta-analysis (Simmonds, Pekar, & Mostofsky, 2008). Previous work in human lesion studies has shown the involvement of the frontal cortex (Godefroy & Rousseaux, 1996), with more specific localisation in the superior medial (Drewe, 1975; Floden & Stuss, 2006; Picton et al., 2007) and right inferior prefrontal cortices, the insula, the dorsal medial frontal cortex (including the supplementary and pre-supplementary motor areas) (Aron, Fletcher, Bullmore, Sahakian, & Robbins, 2003; Chambers et al., 2006). Neuroimaging studies of response inhibition, using fMRI, reliably show frontal lobe activation (Blasi et al., 2006; Garavan, Ross, & Stein, 1999; Liddle, Kiehl, & Smith, 2001; Mostofsky et al., 2003; Rubia et al., 2001; Wager et al., 2005; Watanabe et al., 2002). Although electroencephalography (EEG) and magnetoencephalography (MEG) are limited in spatial resolution compared to fMRI, electrophysiological recordings are far better suited to resolving the temporal dynamics of different stages of inhibitory processing given its fine temporal resolution. For example, event-related potential (ERP) studies offer unique insight into the precise millisecond time scale of the neurophysiological correlates of response inhibition (Albert, López-Martín, Hinojosa, & Carretié, 2013; Bokura, Yamaguchi, & Kobayashi, 2001; De Sanctis et al., 2014; De Sanctis et al., 2020; Falkenstein, Hoormann, & Hohnsbein, 1999; Falkenstein, Hoormann, & Hohnsbein, 2002; Huster et al., 2013; Krakowski et al., 2016; Malcolm et al., 2015; Malcolm et al., 2019; Nieuwenhuis, Aston-Jones, & Cohen, 2005; Nieuwenhuis, Yeung, Van Den Wildenberg, & Ridderinkhof, 2003; Wakim et al., 2021). Furthermore, improved spatial resolution can ultimately be achieved by using higher density electrode arrays combined with source localisation techniques (Gonçalves, Whelan, Foxe, & Lalor, 2014; Leavitt, Molholm, Ritter, Shpaner, & Foxe, 2007; Murray et al., 2002; Pascual-Marqui, Michel, & Lehmann, 1994; Saint-Amour, De Sanctis, Molholm, Ritter, & Foxe, 2007; Strik, Fallgatter, Brandeis, & Pascual-Marqui, 1998).

In the conventional Go/NoGo paradigm, participants are presented with two types of cue stimuli (Go and NoGo cue trials) that are sequentially and randomly presented with either constant or variable inter-stimulus intervals. Task instructions are to respond as quickly and accurately as possible with a button press following Go cues (presentation of a novel stimulus) and withhold the

button press response to the NoGo cues (repetition of previous stimulus). Go stimuli are typically presented more frequently (85-88%) in order to build a prepotent response tendency, thereby increasing the inhibitory effort necessary to successfully withhold a response to NoGo stimuli. Canonical ERP components measured in the Go/NoGo tasks have consistently revealed stimulus locked N2 and P3 ERPs to be larger and to be distributed more frontally in the NoGo compared to the Go trials. In addition, the difference wave, which yields the N2 and P3 voltage difference (i.e., NoGo minus Go, N2d and P3d), is often used to quantify the Go/NoGo response inhibition effect. These components quantify two aspects of inhibitory control, specifically premotor response inhibition or conflict monitoring (N2) and 'finalization' of the inhibition process (P3) (Gajewski & Falkenstein, 2013; Jodo & Kayama, 1992; Kropotov, Ponomarev, Hollup, & Mueller, 2011; Nieuwenhuis et al., 2003). These differences consist of a frontal negativity in a time range of about 200 to 300 ms after the stimulus (N2), and a fronto-central positivity in a time range of about 300 to 500 ms after the stimulus (P3) (Eimer, 1993; Falkenstein et al., 1999; Fox, Michie, Wynne, & Maybery, 2000). Several studies report a right hemifield dominance for the N2 (Filipović, Jahanshahi, & Rothwell, 2000). Together these response inhibition components form part of the inhibition neural network that also involves the dorsomedial and ventrolateral PFC as well as the insula, pre-supplementary motor areas and the anterior cingulate cortex (Baumeister et al., 2014; Huster, Westerhausen, Pantev, & Konrad, 2010; Ridderinkhof, Van Den Wildenberg, Segalowitz, & Carter, 2004). Notably, the latter is also substantially involved in error processing (Ridderinkhof et al., 2004; Taylor, Stern, & Gehring, 2007).

Failures to properly inhibit the response to NoGo cues leads to response errors and can provide insight into post-error action control. Following error commission two types of behavioral changes are observed: post-error slowing (PES) and post-error accuracy improvement (PAI). The PES is characterized by slowing of response speed (reaction time, RT) compared to RTs observed during a sequence of correct button presses (Danielmeier & Ullsperger, 2011; Rabbitt, 1966). There are three hypotheses proposed to account for PES; 1) the cognitive control account describes the PES as the result of increased top-down control (Kerns et al., 2004), 2) according to the orienting account, PES emerges after any kind of infrequent event (Ridderinkhof, 2002), and 3) by the inhibitory account, PES is supported by increased inhibition in trials following error commission. (Notebaert et al., 2009). There remain inconsistent findings in the literature with evidence in favor of the different accounts. In sum previous ERP studies that have investigated post-error adjustments demonstrate an association between PES and on or two of the canonical error-related potentials (Ne and Pe). Though, consistently reported is the direct relationship between any decision-making behavior being "primed" by preparatory activities and the motor response (Band, Ridderinkhof, & van

der Molen, 2003). Recently, is have been argued that error commission leads to neural adjustment mechanism that regulate post-error performance and it is these adjustments that offer more insight into the investigation of post-error neural adjustments than error-detection activities alone and may be more relevant in clinical research (Perri, Berchicci, Lucci, Spinelli, & Di Russo, 2016).

Research on lifespan investigations on response inhibition are sparse and the effects of age on response inhibition related ERPs is unclear. Some studies show that elderly participants suffer from generic inhibition deficits and are unable to perform inhibition-related tasks as well as younger adults (Bokura, Yamaguchi, Matsubara, & Kobayashi, 2002; Hasher & Zacks, 1988; Lucci, Berchicci, Spinelli, Taddei, & Di Russo, 2013; Pires, Leitão, Guerrini, & Simões, 2014; Schmiedt-Fehr, Mathes, Kedilaya, Krauss, & Basar-Eroglu, 2016; Vallesi, 2011; Vallesi, Stuss, McIntosh, & Picton, 2009). Others have shown a lack of performance deficits and argued that the elderly may develop strategies to compensate for reduced inhibitory processes (Cabeza, Anderson, Locantore, & McIntosh, 2002; Hsieh & Fang, 2012; Hsieh, Liang, & Tsai, 2012; Phillips & Andrés, 2010; Tamm, Menon, & Reiss, 2002; Vuillier, Bryce, Szücs, & Whitebread, 2016). However, various methodological differences could contribute to discrepancies in the literature. For example, Go/NoGo tasks have been shown to be more sensitive to age related differences than other response inhibition tasks (Bokura et al., 2002; Lucci et al., 2013; Pires et al., 2014; Vallesi, 2011; Vallesi et al., 2009), suggesting that task specific parameters may be critical to strategies adopted by older adults (Rey-Mermet & Gade, 2018). Developmental studies suggest that by age 7 children conceptually understand when to inhibit a response (Dowsett & Livesey, 2000). Improvements in inhibitory control correspond with increasing metacognitive abilities and general maturation of brain regions thought to underlie executive control, and, in particular, the prefrontal cortex (Carver, Livesey, & Charles, 2001; Harnishfeger & Bjorklund, 1993; Zelazo, Frye, & Rapus, 1996). After 7 years of age there are marked developmental gains in the ability to inhibit prepotent responses throughout childhood that continue into early adulthood (Band, van der Molen, Overtoom, & Verbaten, 2000; Harnishfeger & Bjorklund, 1993; Schachar & Logan, 1990; Williams, Ponesse, Schachar, Logan, & Tannock, 1999). For instance, response inhibition reaction time (RT) improves between age 6 and 20 (Band et al., 2000; Williams et al., 1999). The current dataset affords us the ability to further explore some of these general effects across age groups.

Despite extensive use of the Go/NoGo paradigm, there remains a lack of evidence regarding the impact of core design parameters, including Go/NoGo ratio, inter-stimulus interval (ISI), stimulus duration, and percentage of Go stimuli on the effects of underlying neural mechanisms and how these are manifested in neurophysiological recordings. Some research has focused on task parameter manipulation effects or compared various methodological

differences between variants of the Go/NoGo paradigm. These studies show that even small task manipulations may have large effects on performance. For example, short ISIs also led to faster RTs in and usually coincided with lower accuracy on NoGo trials (Jackson & Balota, 2012; Smallwood et al., 2004; Zamorano et al., 2014). Additionally, there are inconsistencies in the literature on conflict adaption or post-error action control (Event-related negativity; ERN) changes associated with age, perhaps an indication of the wide variability in the sampling procedures and sample sizes. Previous reviews have shown that typically neuro-psychology studies are underpowered in a manner such that statistical effects are likely overestimates of the true effect size and not likely to replicate (Button et al., 2013). Reliability of error-related neurophysiological measure will vary as a function of the number of error trials and the sample size included in the average. Unfortunately, systematic investigations of the number of events and participants required to achieve stability in error-related processing are sparse, and none have addressed variability in sample size. Increasing the sample size reduces the possibility of false positive findings—particularly for small effects like conflict adaptation effects. Given that conflict adaptation and cognitive control are a relatively new areas of research, variability in findings between studies is expected. The goal of the current study is to provide data compiled from a large sample of healthy participants, resampled iteratively to demonstrate the relative stability of measures of error-related brain activity given a range of sample sizes and event numbers included in the averages. To this end our current data repository offers a unique opportunity to further explore the effects these subtle paradigm differences can have on electrophysiological and behavioral outcomes.

Table 1. Summary of Studies included in data repository.

Site	Lab	Set AS	FS	Display	Viewing Distance	Stim Duration	Average Blocks (trials)	Approx. % NoGo	ISI	Visual Angle	Stimuli
Wakim et al. *(2021)*	EMSR	B-256	512 Hz	LDC -1	95 cm	60 ms	1 (8952)	14%	950 ms	8.6° x 6.5°	P+, N, N-
Francisco et al. (2020)	EMSR	B-65	512 Hz	LCD -2	80 cm	600 ms	3 (540)	12%	350-450 ms	8.6° x 6.5°	P+, N
Wilson et al (2017)	EMSR	B-128	513 Hz	LCD -3	80 cm	800 ms	8 (478)	14%	600-650 ms	8.6° x 6.5°	P+, N
Morie et al. (2014)	EMSR	B-160	512 Hz	LCD -4	80 cm	800 ms	7 (180)	15%	200 ms	8.6° x 6.5°	N
Patelaki et al (*in prep)*	MoBiLAB	B-64	2048 Hz	Proj -1	1.5 m	60 ms	7 (240)	13%	950 ms	28° x 28°	P+, N, N-
De Sanctis et al. (2014)	MoBiLAB	B-64	2048 Hz	Proj -3	1.5 m	600 ms	4 (550)	15%	800-1000 ms	28° x 28°	N
De Sanctis et al. (2020)	MoBiLAB	B-160	2048 Hz	Proj -2	1.5 m	600 ms	5 (180)	15%	800-1000 ms	28° x 28°	N, P+
De Sanctis et al. (2016)	MoBiLAB	B-64	512 Hz	LCD -2	1.5 m	600 ms	5 (180)	15%	800 ms	28° x 28°	P+, N, N-
Malcom et al. (2015; 2017)	MoBiLAB	B-64	512 Hz	Proj -2	1.5 m	600 ms	4 (550)	15%	800-1000 ms	28° x 28°	N, P+
De Sanctis et al. (in Prep)	MoBiLAB	B-160	513 Hz	Proj -2	1.5 m	600 ms	5 (180)	15%	800-1000 ms	28° x 28°	XY

Notes: ERMS (Electromagnetically shielded room), MoBiLAB (*see methods*) | Presentation keys: MoBiLAB Screen 1 (Projected centrally (InFocus XS1 DLP, 1024 × 768 pxl), Mobi Screen 2 (Projected centrally (InFocus XS1 DLP, 1024 × 768 pxl) , LCD monitor 1 (Acer Predator Z34, 34") , LCD Monitor 2 (ViewSonic VP2655WP, 34 "), Mobi Screen 3 (InFocus XS1 DLP, 1400 × 1050 pxl). Stimuli: International Affective Picture System (IAPS, *see methods*), p+ (positive), N (Neutral), N- (Negative). XY Optical flow (*see methods*)

5 Materials and Methods

5.1 Data Repository

EEG data presented in this paper were collected across two sites: The University of Rochester Medical Center (UoR) and The Albert Einstein College of Medicine (EinMed). Only EEG recordings from healthy subjects are included and data consist of both previously published and unpublished data from both sites (De Sanctis et al., 2014; De Sanctis et al., 2020; Francisco et al., 2020; Krakowski et al., 2016; Malcolm et al., 2015; Malcolm et al., 2019; Morie, Garavan, et al., 2014; Patelaki et al., 2022; Wakim et al., 2021). Data that were part of Mobile Brain/Body Imaging (MoBI) studies include only the sitting conditions in those experiments. Recently, increased efforts for Open Science and data sharing have resulted in a definition of standard data representation of neuroimaging data, specifically Brain Imaging Data Structure (BIDS), which aims to facilitate the sharing of data and aid scientific reproducibility (Gorgolewski et al., 2016). To this end, EEG data are organised in a specific directory structure, using well-defined file naming conventions and in a standardized data format. All published datasets are de-identified and are archived and organised according to standards and guidelines following the BIDS format. Study files were converted to EEG-BIDS with Fieldtrip Toolbox (Oostenveld, Fries, Maris, & Schoffelen, 2011) (RRID:SCR_004849), using the function data2bids running MATLAB (The MathWorks). To facilitate data sharing, guidelines and agreements for collaboration were established under the guidance of site-specific institutional review boards (IRBs). A list of the included datasets (both published and unpublished) from the selected studies are detailed in Table 1.

5.2 Participants

Demographic information can be found in table 2. Written informed consent was obtained from all participants and studies were approved by the individual institutional review boards at UoR and EinMed for those participating at each site respectively. Participants reported no hearing impairments, developmental and/or educational difficulties or delays, neurological disorders or problems and absence of psychotic symptoms or of any other psychiatric diagnosis. Participants received monetary compensation for their time participating in the respective studies. All procedures employed were compliant with the tenets laid out in the Declaration of Helsinki for the responsible conduct of research. Participants were grouped into three age groups; young age group (YA: 9-17), Middle age group (MA: 18-60), and older age group (OA: 61-90).

Table 2. Datasets grouped into nine studies

Study Groups	Study ID	Subjects selected	Age Range Mean (SD)	Range	Gender M (F)	Site
Patelaki et al (2021)	1	32	42.74(24.36)	18-79	25(14)	UoR
Francisco et al. (2020, prep)	2	75	21.90(9.81)	9-50	31(44)	EinMed
Wilson et al (2018)	3	14	18.51(3.83)	10-25	12(15)	EinMed
Wakim et al. (2021)	4	21	42.25(12.38)	19-65	17(22)	UoR
Morie et al. (2014); Wilson et al (2017)	5	39	41.85(23.91)	19-30	22(17)	EinMed
De Sanctis et al. (2020); Malcom et al. (2015;2017)	6	24	33.71(5.10)	26-50	10(14)	EinMed
Krakowski et al. (2016)	7	33	23.41(3.32)	19-30	13(20)	EinMed
De Sanctis et al. (prep)	8	28	71.41(4.11)	65-79	16(12)	EinMed
De Sanctis et al. (prep)	9	36	45.55(4.05)	21-71	19(17)	EinMed

Notes: Studies groups into 9 Study IDs and consist of both published and unpublished (prep) data.

5.3 Stimuli and experimental procedure

For study specific details on the exact procedures and stimuli used for each study we refer the reader to the Methods sections of the respective published work (*See* Section: Repository and Table 1.) and to the supplementary section for details on unpublished work. Here we give a general overview of the main experimental procedures and stimuli used across the two sites and all studies. Hardware is generally grouped into those studies using MoBI EEG labs and those conducted in standard EEG testing booths (electromagnetically shielded room, EMSR). Participants performed a Go/NoGo task which required them to respond as quickly and accurately as possible to every novel stimulus presentation while withholding responses to the second instance of a repeated image. Depending on the study, stimuli consisted of a combination of or all the following; Positive, neutral and/or negatively valanced pictures from the International Affective Picture System (IAPS) (Lang, Bradley, & Cuthbert, 1997). These pictures are based on normative photographs depicting people, landscapes, abstract patterns, and objects and were presented in a pseudorandomised order. Although, previous research has investigated differences in response inhibition as a function of a stimulus' emotional valence or semantic content, we did not present any data on this as it is beyond the scope of the current paper. The probability of Go and NoGo trials varied across studies but generally set at 85% and 15% (±2%), respectively.

It is important to note here the distinction between the two types of test conditions, EMSR and MoBI. EinMed labs used audiometric grade, sound attenuated and electromagnetically shielded booths (IAC Acoustics, North Aurora, IL. 120A-Series), while MoBI experiments involve recording neurophysiology from an EEG system and movement kinematics from a motion capture system (Gramann et al., 2011; Makeig, Gramann, Jung, Sejnowski, & Poizner,

2009). Typically, MoBI experiments require participants to move during EEG data collection and are designed specifically to investigate interactions of cognition and motoric systems. However, often seated or non-movement blocks (i.e., similar to standard EEG testing conditions) are included in these experiments for comparison. It is these seated control conditions that are included as part of the data repository making possible direct comparisons across test conditions and locations. For more information we direct the reader to the relevant papers listed in table 1. Stimuli were presented centrally against a black background. Table 1 lists study specific information relating to stimulus parameters. For analyses studies are grouped by age of participants or were categorized according to the length and constancy of the inter-stimulus-interval (ISI). There were four ISI categories: long-fixed, short-fixed, long-jittered and short-jittered. The duration of ISI varies across experiments from as little as 350 ms to 3000 ms (for example; (De Sanctis et al., 2014; De Sanctis et al., 2020; Francisco et al., 2020; Garavan, Ross, Murphy, Roche, & Stein, 2002; Krakowski et al., 2016; Morie, Garavan, et al., 2014). These manipulations are manifested as quantifiable changes in neurophysiological recordings, such as changes in ERP morphology and/or location functional brain regions and behaviorally as measured by changes in RTs and commission error data. This is important as there are implications for the relationship between the task and the underlying construct it is intended to measure.

5.4 Behavioral analysis

Reaction time (RT) data were recorded with a precision of 0.1 milliseconds at both sites. Only trials with RTs between 116.7 ms and 1200 ms post stimulus were used for analysis. Data were divided into cases during which participants correctly withheld responses on NoGo cue trials (Correct Rejection, Cr) or correctly responded to non-repetition trials Go cue trials (Hits), or trials on which subjects incorrectly responded to NoGo cue trials (False Alarms, FA). Only hits and correct rejection trials preceded by a hit trial were included (or as otherwise stated). D-Prime (d') also known as the sensitivity index (Green & Swets, 1966; Macmillan & Creelman, 2004) was calculated as the difference between the standardized (z) values of the proportion of hits and the standardized value of the proportion of false alarms. D-prime provides a more reliable indication of response inhibition ability in which hit rate is corrected for the false positive rate $d' = z(H) - z(F)$. Response criterion was calculated as the normalized sum of hit and false alarm rates using the equation; $c = -0.5\left[z\left(P(\gamma|s)\right) + z\left(P(\gamma|n)\right)\right]$. The criterion provided information about the participants' response bias in responding or withholding a response, with either a more conservative or liberal bias across trials. A more conservative bias corresponds to positive criterion values. Instead, a more liberal bias corresponds to negative criterion values.

5.5 EEG acquisition and preprocessing

All data were collected using an ActiveTwo system (BioSemi). Table 1 contains study specific information regarding different channel montages and sampling rates. Offline, the data were bandpass filtered between 0.1 and 35 Hz using a Chebyshev Type II filter (order 54, cutoff 0.5Hz for high pass filtering and 8.5Hz for low pass filtering). Passband attenuation was set to 1dB and stopband attenuation was set to 60dB (high pass) and 80dB (low pass). Several artefact and channel rejection procedures were employed. After filtering, the continuous data were downsampled to 256 Hz. Bad channels were detected automatically based on joint-probability, kurtosis, covariance and were verified by visual inspection of topographical plots. A channel was characterized as “bad” and having excessive noise (low recording signal-to-noise ratio) when the standard deviation (SD) of the time series of that channel compared with that of all surrounding channels exceeded more than 2.5 standard deviations (joint-probability, kurtosis) and 2 SD from neighbouring channels (joint-probability, covariance). Channels contaminated by noise and removed were recalculated by spherical spline interpolating the surrounding clean channels using custom code and functions from Fieldtrip Toolbox. Then, the EEG datasets with excessive noise or unrelated task activity were further denoised using the blind source separation technique, Denoising Source Separation (DSS) (de Cheveigné & Simon, 2008). Next, data were re-referenced offline to the common average. Triggers indicating the start of each trial were sent by the stimulus presentation computer and included in the EEG recordings to ensure synchronization. Trials were either stimulus-onset-timelocked (separately for hits and correct rejections) or response-timelocked (to the motor response to a false alarm trial) between -100 to 900 ms. Epochs were baseline corrected between -100 to -10 ms (blank screen) during the prestimulus interval except for the response-time locked epochs, where baseline was the 100 ms prior to when the motor response was recorded. An automatic artefact rejection threshold of 85 uV was used to eliminate trials containing eye movements, blinks, or electrical artefacts. An additional artefact rejection threshold was calculated based on an array of maximum amplitudes for each trial (the largest absolute value recorded in each epoch across all channels). Epochs containing values > 3 SD from the median of this array of maximum values were removed.

5.6 Automatic independent component analysis

The final preprocessing stage used automatic independent component analysis (ICA) referred to as ICLabel, which is a pre-trained neural network based on the power spectra and spatial distribution of the ICs (Pion-Tonachini, Kreutz-Delgado, & Makeig, ICLabel: An automated electroencephalographic independent component classifier, dataset, and website,

2019). ICLabel training is performed on a dataset containing over 200,000 ICs from more than 6000 EEG recordings (Pion-Tonachini, Kreutz-Delgado, & Makeig, The ICLabel dataset of electroencephalographic (EEG) independent component (IC) features, 2019). Briefly, a single dipole is fit to each independent component (IC) weights topography and the ICLabel extension for EEGLAB is used to classify ICs into seven categories each added to the comp_info annotation structure as “brain”, “eye”, “muscle”, “heart”, “chan_noise”, “line_noise”, and “other”. Classification of ICs into the phenomena that they capture is typically achieved by expert review considering multiple properties (e.g., topographies, spectral analysis, dipole fit) of the ICs. We performed ICA on the “clean” preprocessed data as outlined above. Research has shown that optimal ICA decomposition is achieved between 1-2 Hz highpass filtered EEG data, which results in increased SNR (Viola, Debener, Thorne, & Schneider, 2010; Winkler, Debener, Müller, & Tangermann, 2015). However, while highpass filtering may remove noise from the data and is optimal for IC decomposition, filtering is known to remove relevant information in both early and late ERP components (Acunzo, MacKenzie, & van Rossum, 2012; Rousselet, 2012; Tanner, Morgan-Short, & Luck, 2015). Therefore, in order to achieve both optimal ICA decomposition and retain task related neural information, we computed the ICA (ICLabel) mixing matrix on the “clean” preprocessed data filtered between 1-40 Hz, the artefact components were then discarded and the EEG components were back projected onto the 0.01-40 Hz filtered “clean” preprocessed data, thereby reconstructing an artefact-free signal (Hyvärinen & Oja, 2000; Winkler et al., 2015).

5.7 Common space interpolation across datasets

Finally, by means of interpolation, all EEG datasets were reduced to a common electrode space of a 64-channel montage (BioSemi 10/20 layout). We chose a 64-channel layout as this was the lowest channel number across all the datasets. To do this, the neighborhood structure of each dataset was defined, and a weighted-average of nearest-neighbours interpolation was used to systematically reduce channels down to a 64-channel montage for each dataset with headcaps larger than a 64-channel layout. Original montages of each dataset are available in the data repository. Subsequent analysis was performed using Fieldtrip Toolbox (Oostenveld et al., 2011) (RRID:SCR_004849) in combination with custom-written code and routines.

5.8 Response Inhibition related ERPs

Here the focus is on the main response inhibition ERP components. The negative N2 ERP component has been extensively studied and is associated with successful response inhibition during the Go/NoGo paradigm (Bokura et al., 2001; De Sanctis et al., 2020; Donkers & Van Boxtel, 2004; Eimer, 1993; Falkenstein et al., 2002; Garavan et al., 2002; Katz et al., 2010;

Morie, Garavan, et al., 2014). Both the N2 and P3 were measured at CPz, unless otherwise reported, for both correct rejections (i.e., successfully withheld responses to a repeated image; CR hereafter) and hits (button presses in response to unique images). Error-related negativity (ERN) was measured at FCz, and error-related positivity (Pe) was measured at CPz, from the response-locked ERP to False Alarms (FAs; trials on which a response was made when it should have been withheld). Using the grand averaged waveforms and scalp topographic distributions, four-time windows were defined to capture these components: 160–220 ms (N2), 300–400 ms (P3), 0-80 ms (Ne), and 100-200 (Pe). Next, visual sensory ERPs the P1 (90-130 ms) and P2 (230 280 ms) were measured at bilateral electrodes PO7 and PO8 for hits only. For further analyses on these components, mean amplitude over the respective time windows of interest were extracted and which were chosen based on a mass univariate approach (see Statistics section below). Specifically, Monte-Carlo non-parametric cluster-based statistics was used to inform selection of time windows for further analyses (Clayson, Baldwin, & Larson, 2013; Groppe, Urbach, & Kutas, 2011; Luck & Gaspelin, 2017; Oostenveld & Maris, 2007). Although this approach is fairly conservative the chosen windows align with those reported in the literature. Mean data were used for both between-groups statistics and robust correlation analysis (Pernet, Wilcox, & Rousselet, 2013).

5.9 Connectivity Analysis

Debiased weighted phase lag index (dwPLI) was used to estimate the spectral connectivity between channel pairs. The dwPLI, a measure of phase relationships, is an estimator of sensory level connectivity that is more robust and partially invariant to volume conduction in comparison to other estimators (Peraza et al., 2012). In the current study, the dwPLI measure was computed to estimate the functional connectivity between electrodes (Vinck et al., 2011) using the FieldTrip toolbox in MATLAB (Oostenveld et al., 2011). First the cleaned epoched EEG time series data were decomposed into their time-frequency representations with custom written Matlab code, by convolving them with the set of Morlet wavelets with frequencies ranging from 1 to 35 Hz in 25 logarithmically spaced scaled steps. These complex wavelets were created by multiplying perfect sine waves, here $e^{i2\pi ft}$ denotes the sine wave (where i is the complex operator, f is the frequency (ranging from 1 to 50 Hz) and t is time), with a Gaussian, denoted here as $Gaussian = e^{-t^2/2s^2}$, where s is the width of the Gaussian. The width of the Gaussian ranged from 3 to 12 cycles ($s = c / (2\pi f)$, where c is the number of cycles- specified to have a good trade-off between temporal and frequency resolution. Next, the fast Fourier transform (FFT) was applied to both the EEG data and the Morlet wavelets, these were then multiplied in the frequency domain, then the inverse FFT was applied. Then from this resulting complex signal Z_i Z_i and estimate of frequency specific power at each time point was defined as

$[real(Z_i)^2 + imag(Z_i)^2]$, and an estimate of frequency-specific phase at each time point was defined as $\arctan[imag(Z_i) / real(Z_i)]$. Trial averaged power was decibel normalized $[dB\ Power_{tf} = Log10(Power_{tf} / Baeline\ Power_f)]$, where for each channel and frequency the condition specific power signal during the interval of -100 ms to -10 ms relative to standard stimulus onset served as baseline activity. Inter-trial phase clustering (ITPC) reflects the consistency of phase angles over time across trials, which was calculated by averaging the phase vectors over trials:

$$ITPC_{tf} = \left|\frac{1}{N} * \sum_{n-1}^{N} e^{i(\emptyset_{tf})}\right|$$

where N is the number of trials, n is the trial index, and φ is the phase angle at a particular time-frequency point, ITPC can range from 0 (no phase clustering over trials) to 1 (perfect phase clustering over trials) for each time-frequency point. Next, to estimated inter-site phase clustering we used debiased weighted phase-lag index (dwPLI (Vinck, Oostenveld, Van Wingerden, Battaglia, & Pennartz, 2011), but also see (Stam, Nolte, & Daffertshofer, 2007)), which is a measure of phase-based functional connectivity between regions on the scalp. Depending on the analyses, the absolute value of the sum (over either trials or over time), of the sign of phase angles of the channels is taken, the PLI metric reflects the degree to which the time series at two channels show asymmetry in the distribution of phase leads and lags. In doing so it partials out random as well as zero phase-lag, thereby controlling for spurious inflated connectivity due to volume conducted common source activity (also, field spread) (Nunez et al., 1997). Here, the debiased weighted version of the PLI (dwPLI) in addition weights the phase angle difference vectors according to their distance from the real axis, and controls for a positive bias for low PLI values (Vinck et al., 2011). In the current study we adapt the dwPLI function as implemented in Fieldtrip toolbox (Oostenveld et al., 2011) for Matlab using custom code and routines written in Cohen (2014). We first applied the summation over trials for the group-level analyses across condition-averaged results.

5.10 Statistical analysis

Linear Mixed Effects Model

Linear mixed-effects models (LMM) were implemented to analyse behavioral and electrophysiological data, using the *fitlme* function in Matlab using the restricted maximum likelihood (REML) method. Our analyses included both discrete and continuous data across multiple levels, LMM afford the ability to analyse these complex data. Advantages over standard analysis of variance (ANOVA) approaches have been previously reported (Krueger & Tian,

2004; Luke, 2017; Wainwright, Leatherdale, & Dubin, 2007). Where appropriate, variable and factor definitions are reported for the corresponding tests within text. After visual inspection of the residual plots, it was clear there were no obvious deviation from homoscedasticity or normality. All *p*-values were estimated using the Satterthwaite approximations. Post-hoc analyses were performed using linear hypothesis testing on linear regression model coefficients (*coeftest*). Mixed-effects models account for multiple comparisons. To test the effects of RT across age groups as a function of trial order, we used age_group (YA, MA, OA) and trial_order (PreER1, ER, PoER1, PoER2) as fixed factors, subjects as a random factor, and RT as the dependent variable. Post hoc β coefficient tests were run using the Satterthwaite correction. Here we list the resulting linear-model expression for our various analyses: $LME = (RT_{data} \sim 1 + age_{group} + trl_{order} + age_{group} * trl_{order} + (1|Subjects\_ID))$. Next we tested post error-related slowing or action control in RTs post error trials, the resulting linear model expression: $LME = (RT_{data} \sim 1 + RT_{ratio_{trl_{sel}}} + N2\_Amp_{channel} + (1|Subjects\_ID))$.

Estimating Bayes Factor Anova

As well as using frequentist probability-based statistics, we also used the Bayesian analog of an ANOVA (*anovanBF*) to allow us to explicitly determine the amount of evidence in favour of the null hypothesis (H_0: no interaction). We estimated the Bayes factors (BF_{10}) using Matlab code adapted from RStudio (R-Core-Team, 2016; the function *anovanBF* in the toolbox *Bayes factor* (Morey, Rouder, & Jamil, 2015)). We adopted the commonly used Jeffrey-Zellner-Siow (JZS) prior with a scaling factor of 0.707 (Rouder, Morey, Speckman, & Province, 2012; Rouder, Speckman, Sun, Morey, & Iverson, 2009; Schönbrodt, Wagenmakers, Zehetleitner, & Perugini, 2017). Monte-Carlo resampling with 10^6 iterations was used for the BF_{10} estimation. Subjects represented the random factor. Importantly, this estimation allows us to quantify evidence that our experimental factors and interactions explain variance in the data above the random between-subject variations. Standard convention stipulates that any BF_{10} exceeding 3 is evidence in favour of the alternative hypothesis (H_0), while below 1 is in support of the null hypothesis (H_0), and BF_{10} ranging between 1-3 is taken as weak evidence (Wagenmakers, Wetzels, Borsboom, & Van Der Maas, 2011).

Spatio-temporal Statistical Cluster Analyses

Spatio-temporal significance at the group level of ERP evoked response changes were evaluated by a nonparametric cluster-based permutation statistics (Oostenveld et al., 2011; Oostenveld & Maris, 2007). This procedure was further used to determine the loci and time windows of response inhibition related activity, defined statistically by comparing the difference of between Go and NoGo trials. This randomisation procedure uses a cluster-based threshold

correction method to control for the type I error rate in the context of multiple comparisons. This is achieved by identifying clustering neighbours that show significant differences over sensors, time, and/or frequency rather than performing separate tests on each sensor, sample frequency pair. Data were selected where the difference between the two conditions whose sensor- time-pairs t-statistics exceeded the critical p-value of 0.025% for two-sided testing (corrected). The selected sensor- time-pairs were then grouped into clusters wherein each cluster, the sensor-time-pairs form an arrangement that is connected spatially and temporally. Such that, if the sensor- time-pair t-statistics exceeded the statistical threshold were neighbouring spatially and temporally, then these sensor- time-pairs were grouped together as a cluster. Next, each cluster was assigned a cluster-level statistic, calculated by the sum of the sensor- time-specific statistics. That is, the cluster-level statistic is contingent on the size of the cluster and the magnitude of the sensor- time-specific t-statistics within that cluster. To control for the Type-I error rate across all spatiotemporal data, the cluster-level statistics were evaluated under the randomisation null distribution of the maximum cluster-statistic. Therefore, using only the maximum cluster-level statistic as the test statistic, allows the control of the Type-I error rate rather than multiple tests for every sensor- time-pair. By randomizing the data across the two conditions (i.e. Go and NoGo trials) and recalculating the test statistic 5000 times, we obtained a reference distribution of maximum cluster t-values to evaluate the statistic of the actual data (Monte Carlo p-value). The results of these statistics would allow the demarcation of significant time-sensor -frequency clusters to be used as regions of interest (ROI) for further analyses. For testing time-frequency data (ITPC and dwPLI) we performed exploratory cluster-based permutation testing routines as outlined above. Here we either averaged over several time-frequency windows that we selected based on previous literature, our evoked results, and evaluated non-parametrically whether there were channel-clusters of condition differences. In addition, to confirm the spatial specificity of connectivity between our predefined clusters, we also performed a seeded-synchrony analysis with cluster-based permutation testing.

Robust Correlation Analyses

All correlation coefficients and corresponding p-values were computed using Spearman correlation. Correlations resulting in significant p-values were quantified using Robust Correlation (Pernet et al., 2013). This stringently assesses for false positive correlations using bootstrap resampling including six additional validation tests (Rousselet, 2012). Only significant correlations are shown, where significance were corrected for multiple comparisons using a family-wise error rate using maximum statistics through permutation tests (Groppe et al., 2011).

Circular Statistics

For the sliding circular ANOVA, the same method was used as for the standard ANOVA. However, epochs were created around the phase time-series ϕx (the angle of hx) and no baseline correction was performed. Circular statistics were performed using the CircStat toolbox making use of the circular equivalents of the one-way and two-way ANOVA (Watson–Williams test (circ_wwtest.m) and Harrison–Kanji test (circ_hktest.m), respectively). A circular ANOVA attempts to explain the amount of circular variance that is explained by task parameter

6 Results

EEG data were recorded across multiple sites with slight variations on a Go/NoGo paradigm using different channel montages. Participants were required to push a button on Go trials while withholding their response on NoGo trials. Here we compare canonical components reported in the literature and offer some insight into how both age and small variants in task parameters affect cortical responses across the datasets. These data are currently available to download via Dryad at []. Our results here serve to demonstrate the efficacy of the data repository and potential use to other researcher in further research. Participants were further separated into three age groups; young age group (YA: 9-17), Middle age group (MA: 18-60), and older age group (OA: 61-90).

Table 3. Participants' behavioural performance on the Go/No-Go EEG task across 9 grouped studies: D-prime and reaction times.

Study Group	*d*-Prime mean (SD)	Criterion (*c*) mean (SD)	RT hits mean (SD)	False Alarm mean (SD)	RT after FA mean (SD)
1	2.34(0.25)	0.16(0.11)	427.95 (92.34)	495.82 (222.73)	222.73 (229.31)
2	2.11(0.21)	0.51(0.19)	401.09 (61.95)	574.32 (305.42)	305.42 (104.12)
3	1.94(0.09)	0.41(0.13)	410.53 (63.25)	545.15 (276.68)	276.68 (105.96)
4	1.79(0.17)	0.46(0.12)	432.03 (70.35)	559.02 (273.61)	273.61 (105.38)
5	2.00(0.21)	0.65(0.27)	360.85 (32.04)	530.10 (263.38)	263.38 (105.27)
6	2.01(0.18)	0.41(0.08)	388.83 (42.63)	504.41 (256.61)	256.60 (106.08)
7	1.48(0.16)	1.06(0.11)	399.35 (54.42)	490.91 (245.25)	245.25 (105.82)
8	1.89(0.15)	0.36(0.06)	484.94 (59.51)	491.88 (246.75)	246.75 (116.59)
9	1.85(0.91)	0.17(0.23)	540.98 (64.25)	489.71 (222.84)	222.84 (118.19)
Age Groups					
Young	2.34(0.25)	0.16(0.11)	427.95 (92.34)	495.82 (222.73)	222.73 (229.31)
Middle	2.11(0.21)	0.51(0.19)	401.09 (61.95)	574.32 (305.42)	305.42 (104.12)
Older	1.93(0.09)	0.41(0.13)	414.62 (60.57)	547.77 (285.82)	285.82 (105.13)

Notes: Reaction time (RT), Standard Deviation (SD). RT shown in milliseconds.

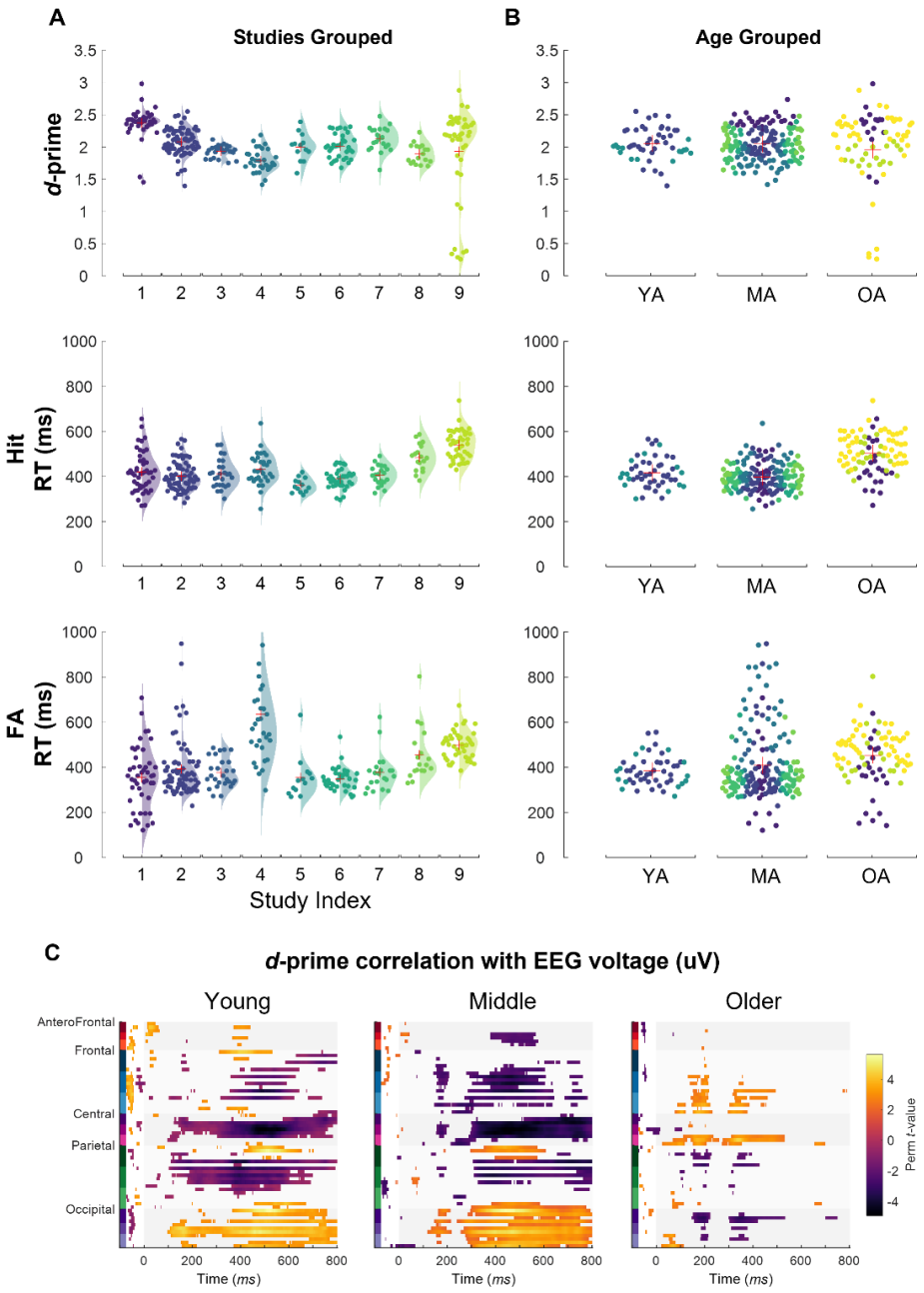

Figure 1. Behavioral performance. (A) D-prime, Hit- and FA-RTs across all 9 datasets. (B), Performance collapsed across all datasets and groups into three age groups (YA, MA, OA) for D-prime, Hit- and FA-RTs from top panel down respectively. Dots represent single subject data with kernel density estimates underlay are colour coded for each dataset. (C) D-prime relationship with EEG voltage across the three age groups. Statistical channel-time cluster plots show significance scores for a cluster-based permutation test (only significant data are shown demarcated by colour; *Nperm* = 5000; $p < 0.05$).

6.1 Behavioral results

To test for differences in behavioral performance across datasets, a two-way ANOVA was used. As expected, there was a main effect of *d-prime* ($F_{(1,302)} = 15.13, p < 0.001, \eta^2 = 0.29, BF_{10} = 4.25\ \mathrm{x}10^{15}$), likely reflecting that some datasets contained mostly OA participants (see Figure, 1B). Post hoc analyses were carried out using Bonferroni-corrected two-sample

independent-means *t*-tests which showed that $study_1$ and $study_7$ were significantly different from all other studies (statistics not reported). Next to test for differences in RT between studies, we used a mixed-effects model (LME). There was an overall main effect of study type ($\beta = 8.59,\ SE = 2.88,\ p < 0.001$), and trial type; for false alarms ($\beta = -37.59,\ SE = 2.88,\ p < 0.001$) and hit trials after FA trials ($\beta = -31.28,\ SE = 4.10,\ p < 0.001$), showing that RTs for FA trials were shorter in general. While Hit trial RTs subsequent to FA trials were longer n latency. Next, there was no significant main effect of *d*-prime across the three age groups (YA, MA, OA) ($F_{(1,302)} = 0.83, p = 0.43, \eta^2 = 0.05, BF_{10} = 0.05$). Using an LME model, we tested for differences in RT between age groups. An overall effect of age group was found for false alarms while controlling for study type ($\beta = 28.73,\ SE = 12.92,\ p < 0.01$), and Hits after FA ($\beta = 40.46,\ SE = 13.81,\ p < 0.01$).

6.2 Response Inhibition: N2 & P3

For the main purposes of the current paper and for brevity, only a selection of channels are shown that represent the main effects and interactions either involving age- or study-related differences. Response inhibition relevant components (N2 and P3) are shown in Figure 2, which shows the data collapsed into three age groups (YA,MA and, OA), while Figure 3, show all the data combined (Gavg). Using cluster-based permutation statistics ($channel \times time$) it is possible to quantify significant response inhibition neurophysiology as a function of temporal and spatial differences across subjects within each age group.

Figure 2B shows cluster plots (expressed in cluster maxsum *t*-statistics) for each group and significant clusters ($p < 0.01$) are shown in colour which are graded according to the permutation t-statistic (*t*-value, Nperm = 5000; see Methods Section). Figure 2A shows the grand averaged ERP waveforms across the three age groups for Go (Hit) and NoGo (correct rejections, Cr) trials at electrode CPz. The lower subplot in Figure2A, shows the corresponsing t-statistics at channel CPz extracted from the cluster-based permutation statistics as presented in Figure 2B. Ultimately, the *t*-value morphology across time here is analogous to the difference waveform. In addition to the ERP waveforms, Figure 2A, shows the corresponsing topographical distribution of the average (Cr-Hit) neural activity differences averaged over the N2 and P3 time-windows (also demarcated in grey) and significant channels are indicated by red markers (based on cluster based statistics). Significant time-points are illustrated with a thick-red line. We found a significant N2 effect at CPz for the YA and OA groups but not for the MA group. However, largely the surrounding channels were significant during this time-window. We found a significant P3 effect across all age groups.

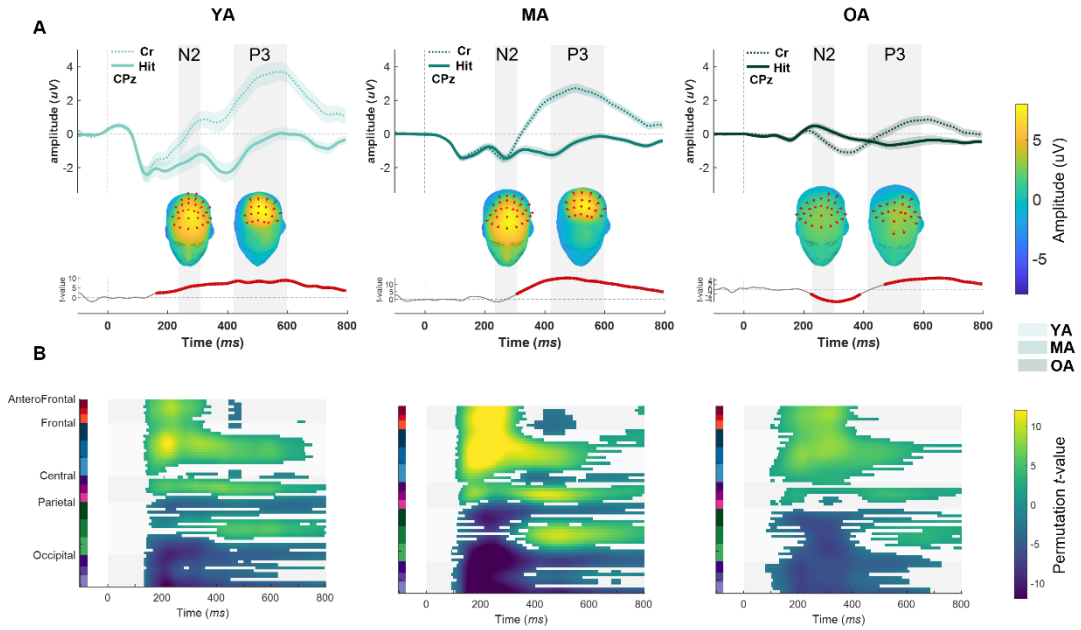

Figure 2. Age related response inhibition N2 and P3 components. (A) Grand-averaged Go/NoGo ERP waveforms across the three age groups for channel CPz (shaded line, SEM across participants). Grey bars demarcate latencies over which the grand average 3D topographical maps were calculated, significant electrodes plotted in red (first level significance at $p < 0.05$, cluster significance at $p < 0.01$ FDR). Subplot shows main effect cluster statistic between Go-NoGo trials (thick red line indicates significant temporal regions, $p < 0.001$). **(B)** Channel-time Statistical cluster plots (expressed in cluster maxsum *t*-statistics), only significant spatio-temporal regions plotted. Positive *t*-values (yellow) indicate Cr trials voltage was higher than Hits.

Next, to test for the presence of significant interaction effects across age groups as a function of trial-type (Cr (NoGo) and Hit (Go)) an initial exploratory cluster-based permutation was used first testing within each trial-type (Figure 3A), next using a mass univariate $(AgeGroup^{\times}Trial^{\times}Chan^{\times}Time)$ approach (Groppe, Urbach, & Kutas, 2011) to test for significant interactions effects across all variables (Figure 3C), and finally we extracted the voltage amplitudes across time-channel windows of interest (N2 and P3 components) and explored these effect more specifically using a Linear-Mixed Effect model (LME). Figure 3A shows the mean ERP waveforms for Cr and Hit trials at channel CPz. The subplot shows the *t*-statistics extricated from the cluster-based permutation test. There is a significant interaction effect across age-groups as a function both time windows of interest over the N2 and P3 components for the Cr trials while the Hit interaction effect is less prominent during the P3 time-window. These results show that there are significant differences in response inhibition electrophysiology across age groups. Figure 3B shows the single subject rain cloud plots of the averaged ERP amplitudes for each group for the Cr trials for both N2 and P3 time-windows. These show that the YA and MA groups had similar mean amplitudes for the N2, while the OA had a slightly smaller negative deflection. While the again both YA and MA groups had similar P3 amplitudes compared to the OA group which had lower amplitude. These statistics are reported in the next section. Finally, Figure 3C (right) shows the interaction results of the mass univariate permutation test. The results how a strong broad cluster across large regions of the sculp around

the N2 component, while there are two electrode clusters of interest around P3 (400 ms) over central and right parietal scalp area. Figure 3C (left), shows data extracted from the cluster plots at CPz. Topographical plots are averaged during the time-window demarcated by the grey bars.

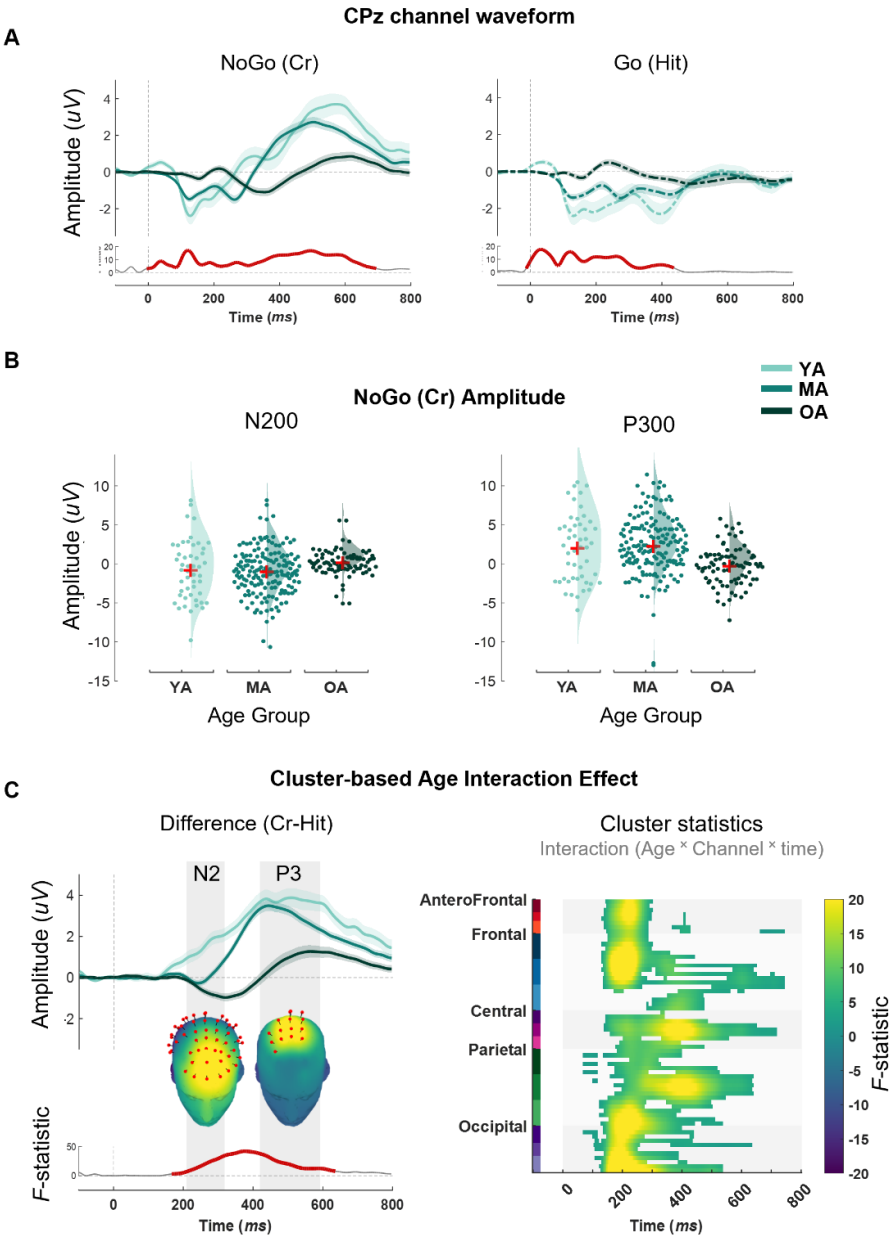

Figure 3. Response inhibition interaction effect across age. **(A)** Grand-averaged Cr (NoGo) and Hit (Go) ERP waveforms across the three age groups for channel CPz (shaded line, SEM across participants). Subplots show cluster *t*-statistics as a function of time, red think line indicates significant interaction effect ($p < 0.01$). **(B)** Raincloud plots of ERP component amplitudes, dots represent single subjects superimposed on the corresponding rain kernel density estimates. **(C) Right,** Channel-time statistical cluster plots of the mass univariate interaction effect (age*channel*time; expressed in cluster maxsum *F*-statistics), only significant spatio-temporal regions plotted. Positive *t*-values (yellow) indicate Cr trials voltage was higher than Hits. **Left,** Corresponding ERP interaction waveforms. Grey bars demarcate latencies over which the grand average 3D topographical maps were calculated, significant electrodes plotted in red (first level significance at $p < 0.05$, cluster significance at $p < 0.01$ FDR). Subplot shows main effect cluster statistic between Go-NoGo trials (thick red line indicates significant temporal regions, $p < 0.001$).

To explicitly test for differences between conditions as a function of age group, Linear-Mixed Modelling (LMM) was used. A full model (linear effects of Go and NoGo P3 amplitudes (400-580 ms positive inflection), Age group plus their interaction) with subjects as random factors was used, while controlling for study group as a factor. There was a significant main effect of effect of age group ($\beta = -3.02,\ SE = 0.45,\ p = 4.41\,\text{x}10^{-11}, BF_{10} = 0.05$), as expected and shown in Figure 2, the P3 amplitude in the NoGo trials (4.42 µV ± 2.25) were significantly larger than in the Go trials (4.42 µV ± 2.25), as indicated by a main effect of P3 amplitude ($\beta = -5.46,\ SE = 0.75,\ p < 0.001, BF_{10} = 0.05$), and an interaction between age group and P3 ($\beta = 1.42,\ SE = 0.56,\ p = 7.75\,\text{x}10^{-08}, BF_{10} = 0.05$). Post hoc analyses revealed that in the NoGo trials, the P3 amplitude was significantly larger in the YA compared to OA ($t_{(125)} = 4.92, p = 2.66\,\text{x}10^{-06}, BF_{10} = 5.72\,\text{x}10^{03}$) and MA and OA ($t_{(251)} = 5.15, p = 5.33\,\text{x}10^{-07}, BF_{10} = 2.51\,\text{x}10^{04}$). Though, there was no significant difference between YA and MA ($p = 0.08, BF_{10} = 0.73$). This is unsurprising as there is a larger gap in age between MA and OA groups.

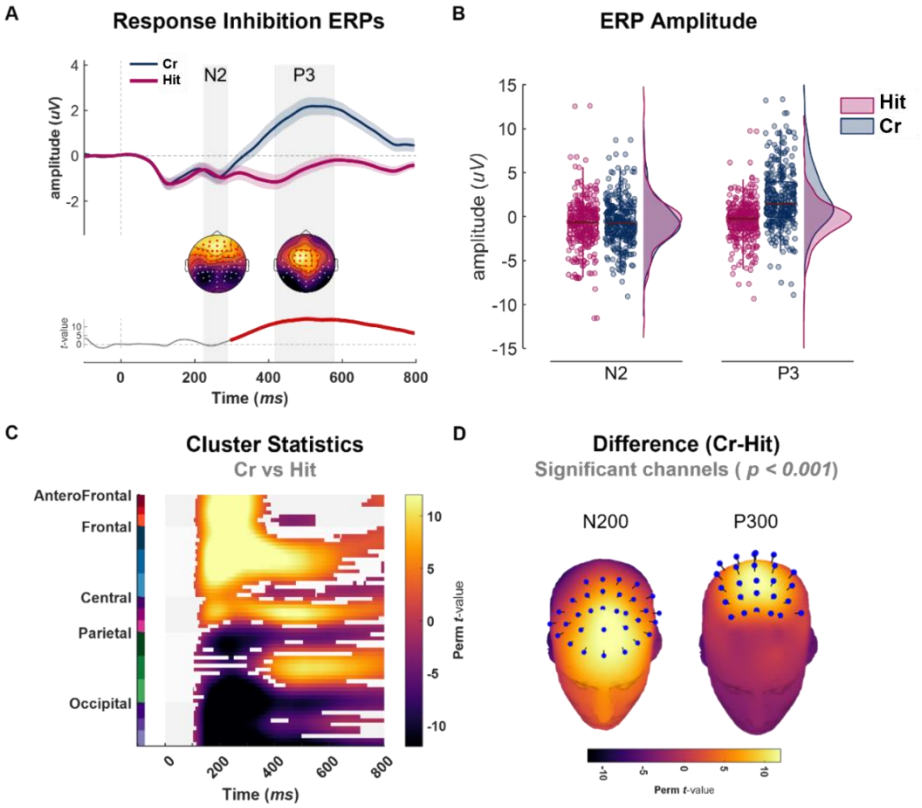

Figure 4. Response inhibition across entire dataset. **(A)** Grand-averaged Cr (NoGo) and Hit (Go) ERP waveforms across the three age groups for channel CPz (shaded line, SEM across participants). Subplots show cluster *t*-statistics as a function of time, red think line indicates significant interaction effect ($p < 0.01$). Grey bars demarcate latencies over which the grand average 3D topographical maps were calculated, significant electrodes plotted in red (first level significance at $p < 0.05$, cluster significance at $p < 0.01$ FDR). Subplot shows main effect cluster statistic between Go-NoGo trials (thick red line indicates significant temporal regions, $p < 0.001$). **(B)** Raincloud plots of ERP component amplitudes, dots represent single subjects superimposed on the corresponding rain kernel density estimates. **(C) Left,** Channel-time statistical cluster plots of the mass univariate interaction effect (age*channel*time; expressed in cluster maxsum *F*-statistics), only significant spatio-temporal regions plotted.

Positive *t*-values (yellow) indicate Cr trials voltage was higher than Hits. **Right,** 3D topographical maps averaged over the N2 and P3 time-windows, significant electrodes plotted in blue (first level significance at $p < 0.05$, cluster significance at $p < 0.01$ FDR).

Using an analysis approach similar to that outlined above, Figure 4 shows the grand averaged data across the entire dataset (n=302). Figure 4A shows the grand-averaged ERP waveforms for Cr and Hit trials at channel CPz. Interestingly there was no significant main effect of response inhibition N2 at CPz (although neighbouring channels show a clear significant effect, see Figure 4C), but we did find a main effect during the P3 time-window. The averaged ERP amplitude of these two time-windows are shown in Figure 4B. Figure 4C shows the cluster-based statistics results and there are clear positive clusters around N2 time-windows in frontal channels, while the statistics show a stronger effect during the P3 time-window at central and right parietal electrodes. Figure 4D shows topographical plots of the cluster-based statistics over N2 and P3 and significant channels are plotted (blue).

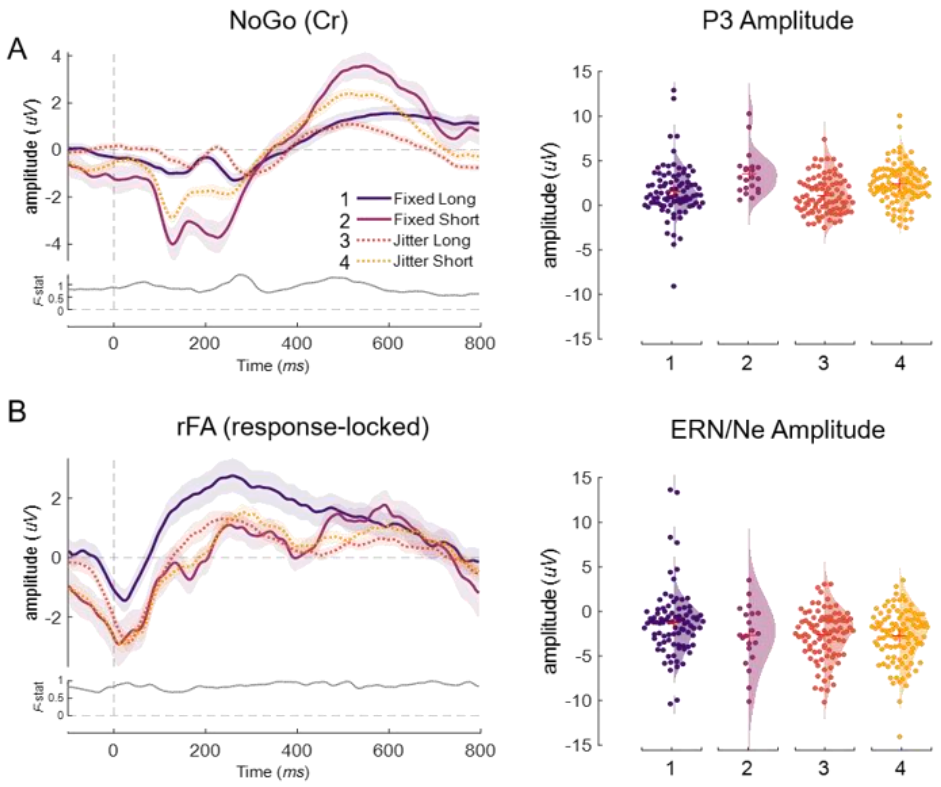

Figure 5. ISI type comparisons. (A) left panel, NoGo ERPs for each ISI types. For the analyses if statistics we controlled for age. Right panel show P3 amplitude averaged data. **(B)** ERN ERPs for the four ISI type conditions. Right panel show averaged ERN amplitudes (0 – 50 ms). Dots in cloud plots represent single subjects with kernel density functions. Shaded line represents SEM. All ERP subplots show there was no significant main effect across all groups (A, B).

6.3 Investigating neurophysiological differences due to task design

The ISI duration type and length was one main distinguishing feature between the different study paradigms. These could be classified into ISI types that were either fixed or jittered and either of short (< 650 ms) or long latency (> 800 ms) periods. To explore any effect of ISI type across the datasets, we collapsed studies into four ISI condition types, Fixed Long (lg-fix), Fixed Short (sh-fix), Jitter Long (lg-jit) and Jitter Short (sh-jit). Using Linear-mixed modelling we found a significant main effect for study type while controlling for age for P3 amplitude at electrode CPz ($F_{(3,245,43)} = 10.013, p = 3.001\,\mathrm{x}10^{-06}$) and we found a significant main effect for ERN/Ne ($F_{(3,245,43)} = 13.142, p = 5.027\,\mathrm{x}10^{-08}$). Interaction effects can be seen in Table 4. One interesting finding from these comparisons is that of the ERN/Ne amplitudes across study ISI types. These yielded by far the most significant effects across study types

.

Table 4. Linear-mixed effects model results (F and *p* values) for N2, P3 and ERN/Ne amplitude across grouped study ISI types

Factors	F value	*p* value	DF(2)
N2 Amplitude			
lg-fix*sh-fix	0.708	4.01E-01	-1.23E+03
lg-fix*lg-jit	3.425	6.59E-02	1.70E+02
lg-fix*sh-jit	10.673	1.30E-03	1.85E+02
sh-fix*lg-jit	4.518	3.44E-02	2.98E+02
lg-jit*sh-jit	4.384	3.72E-02	2.88E+02
sh-fix*sh-jit	2.939	8.76E-02	2.88E+02
P3 Amplitude			
lg-fix*sh-fix	3.616	5.87E-02	1.97E+02
lg-fix*lg-jit	1.129	2.90E-01	1.66E+02
lg-fix*sh-jit	3.920	4.93E-02	1.75E+02
sh-fix*lg-jit	4.513	3.45E-02	2.97E+02
lg-jit*sh-jit	12.347	5.13E-04	2.86E+02
sh-fix*sh-jit	3.481	6.31E-02	2.83E+02
ERN/Ne Amplitude			
lg-fix*sh-fix	21.442	5.87E-06	2.50E+02
lg-fix*lg-jit	24.753	1.60E-06	1.68E+02
lg-fix*sh-jit	61.059	3.94E-13	1.86E+02
sh-fix*lg-jit	25.529	7.61E-07	2.98E+02
lg-jit*sh-jit	29.166	1.39E-07	2.88E+02
sh-fix*sh-jit	34.363	1.23E-08	2.92E+02

Notes: lg - Long, sh - Short, fix - fixed latency, jit - jittered latency. Studies grouped according to long or short ISIs and if these are fixed or jittered intervals. DF - Degrees of freedom, all DF(1) = 1.

6.4 Response-locked ERPs for error NoGo trials: Event-related Negativity (ERN/Ne) and Error positivity (Pe)

To measure neurophysiological correlates of error-related processing, epochs response-locked to FAs (motor responses to NoGo trials) and baselined to the 100 ms period pre-response, were averaged at the individual subject level and submitted to statistical analyses. This typically yields an error related negativity (ERN; aka Ne, for negative error response) that begins close to the motor response and is then followed by an error related positivity (Pe).

Specifically, FA trials here were response-timelocked (rFA) to the motor response rather than aligned on stimulus-onset as in previous analyses. As anticipated, Figure 5B shows a negative deflection associated with error (FA) trials began shortly after response execution and peaked approximately 55 ms later, primarily at the fronto-central regions (Fz, FCz, CPz). For subsequent statistical analyses, we used cluster-based statistics to inform the windows of analyses. Based on the peak ERN latency (55 ms), a window of interest was defined around the most negative ERN deflection peaking between 0 to 150 ms. An LME model with Satterthwaite corrected p values confirmed the presence of an ERN when subjects responded in error ($\mathrm{F}(1{,}302) = 14.24\ \mathrm{p} < .001$). The effects ERN and Pe for the FA trials were tested by fitting an LME with normalized F1 as the outcome variable, with fixed effects of channels (CPz and FCz), subject age, and ERN component and their interaction, with subjects as the random effects. For the effects for ERN/Ne components, there was a significant main effect for; age group ($\beta = 0.04,\ SE = 0.01, p < 0.001, \eta^2 = 0.63, BF_{10} = 3.51\ \mathrm{x10}^{-04}$), and for electrodes ($\beta = 1.82,\ SE = 0.33, p = 7.52\ \mathrm{x10}^{-08}, \eta^2 = 0.61, BF_{10} = 936.41$), and an age-group × electrode interaction ($\beta = -0.02,\ SE = 0.01, p = 0.001, \eta^2 = 0.63, BF_{10} = 8.94\ \mathrm{x10}^{02}$). The ERN/Ne for the OA group had a significantly more negative amplitude than the YA group ($t_{(125)} = -4.69, p = 7.11\ \mathrm{x10}^{-06}, BF_{10} = 2.33\ \mathrm{x10}^{03}$) and MA group ($t_{(244)} = -3.56, p = 4.47\ \mathrm{x10}^{-04}, BF_{10} = 51.86$), and there was no significant difference between MA and YA subjects. Finding no significant difference between the MA and YA might be expected as the age ranges per age-group were small. These results confirm that the difference in the ERN magnitude between correct and incorrect trials was largest at the FCz and Cz recording sites (Figure 6). Our results are consistent with previously reported ERN morphology and topography.

Error positivity (Pe) was defined as the most positive data point in the baseline-corrected window, between the ERN conclusion (150 ms) and 525 ms post response execution. Using spatio-temporal cluster-based permutation testing, Figure 6B shows that Pe had a significant fronto-central scalp distribution, ($\mathrm{F}(2{,}604) = 13.65, p < 0.001$), and was also significantly associated with FA trials compared to Hit trials ($\mathrm{F}(1{,}302) = 45.90, p < 0.001$). Next for the effects for Pe, there was no significant main effect for age group ($\beta = -0.006,\ p = 0.71$), but there was a significant main effect for electrode ($\beta = 1.14,\ SE = 0.41, p = 0.009, \eta^2 = 0.52, BF_{10} = 1.80\ \mathrm{x10}^{05}$) and age group × electrode interaction ($\beta = -0.02,\ SE = 0.01, p = 0.009, \eta^2 = 0.41, BF_{10} = 8.94\ \mathrm{x10}^{02}$). The ERN/Pe was only significant at FCz ($F_{(259)} > 18.41$, $p = 2.42\ \mathrm{x10}^{-05}$), the YA group had a significantly more positive amplitude than the MA ($t_{(125)} = 4.20, p = 1.93\ \mathrm{x10}^{-05}, BF_{10} = 3.53$) and OA ($t_{(244)} = 2.52, p = 0.03, BF_{10} = 3.86$), and there was no significant difference between MA and YA group subjects.

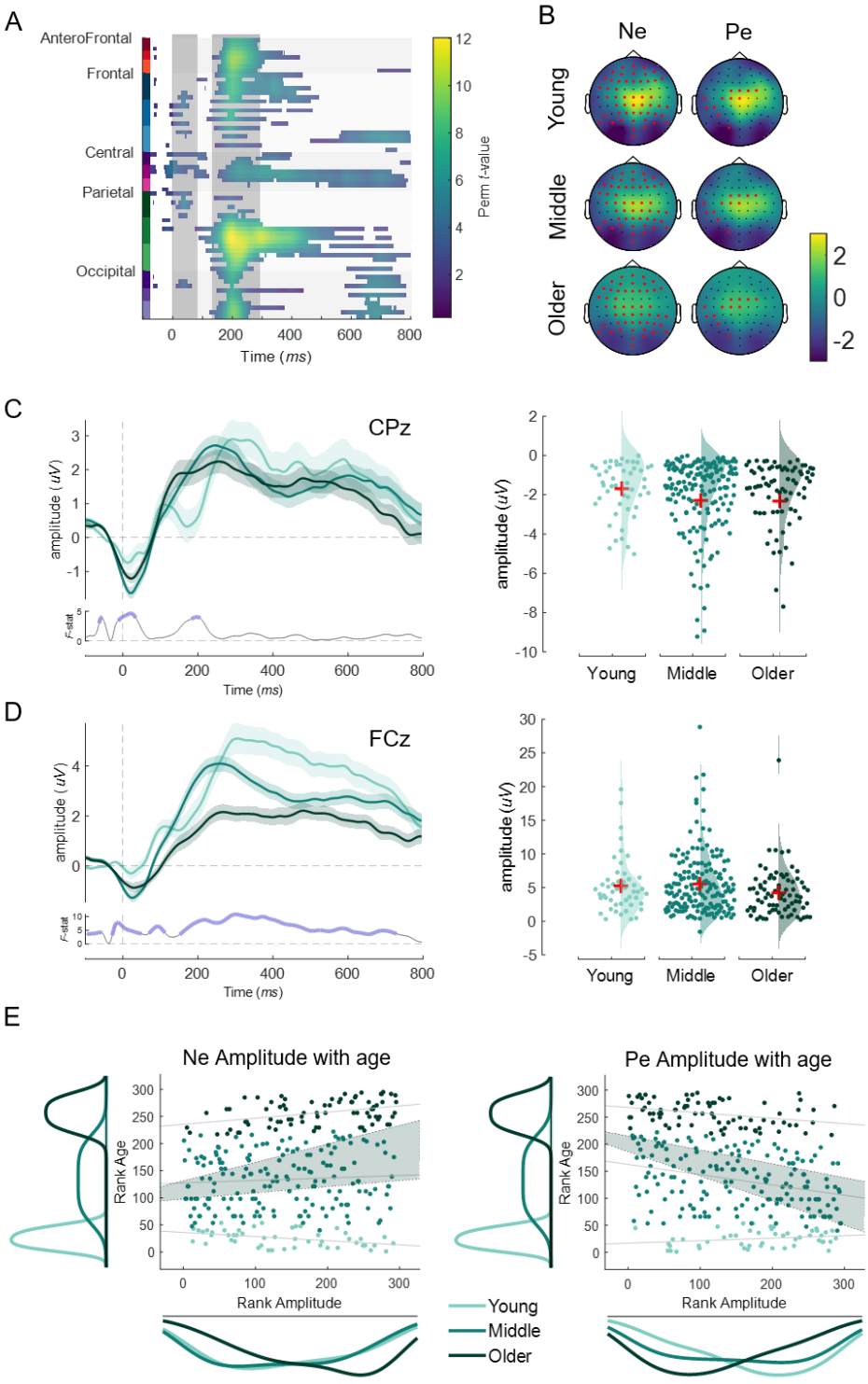

Figure 6. Event-related negativity (ERN). (A) Channel-time cluster plot showing main effect of age groups across ERN trials (only significant data are shown demarcated by colour; *Nperm* = 5000; $p < 0.05$). Grey shaded regions demarcate latencies which the left panel topographical plots have been averaged from. Red dots indicate significant main effect channels. **(C, D; left panel)** ERN (0-50 ms) ERPs for channels CPz (ERN) and FCz (Pe). Shaded line indicates SEM, subplots show cluster statistics (*Nperm* = 5000, thick line shows $p < 0.05$). **Right panel,** averaged ERN amplitudes cloud plots with kernel density plots for the three age groups, dots are single subjects. **(E)** ERN amplitude (CPz) and Pe amplitude (FCz) relationship with age. Robust Pearson's correlations with density curves (bootstrap permutation test $p < 0.05$, confidence interval 95%). All data are colour coded according to group type.

Finally, the relationship between ERN component amplitude and subject age was tested. For this analysis, age was defined as a continuous variable rather than a categorical grouping factor. Specifically, robust correlation analysis with bootstrap resampling (Pernet et al., 2013) was used to check for correlations between these measures across subjects. There was a significant negative relationship between age and ERN/Ne amplitude for CPz ($r_s = -0.21,\ p = 4.14\ \mathrm{x}10^{-04}, 95\%\ CI\ [-0.31 - 0.09]$). YA subjects had significantly larger ERN/Ne amplitudes. There was also a significant negative relationship between age and ERN/Pe amplitude for FCz ($r_s = -0.19, p = 0.001, 95\%\ CI\ [-0.30 - 0.07]$), showing that YA subjects had significantly higher ERN/Pe amplitudes then OA subjects.

6.5 Post-Error Slowing (PeS)

Participants tend to slow down after they commit an error, a phenomenon known as post-error related slowing (PES; aka post-error action control (PEA)). PES was quantified as the difference in RT between post-error trials (PoFA) and the associated pre-error trials (PreFA) using the following method $\widehat{\mathrm{PES}} = \mathrm{RT}_{(\mathrm{PoFA}_1)} - \mathrm{RT}_{(\mathrm{PreFA}_1)}$, which has been shown to be robust to extraneous behavioral adaptation or global task-unrelated fluctuation (Dutilh et al., 2012). Specifically, to behaviorally evaluate PES as a byproduct of post-FA recovery (i.e, PEA), RTs for error NoGo trials (FA), pre-error Go trials (PreFA), and first and second post-error Go trials (PoFA_1 and PoFA_2 respectively) were calculated. PES was examined by comparing temporally adjacent post-error trials with the PreFA trials (Orr & Hester, 2012). Stimulus locked N2 components for the PoFA_1 and PoFA_2 trials with the PreFA trial to examine post-error processing were also compared. Table 5 shows descriptive statistics on error rate and RTs for the PreFA_1, FA, PoFA_1, and PoFA_2 trials. Finally, the relationship between ERN amplitude on FA trials with PoFA_1 and PoFA_2 PES amplitudes were tested.

Table 5. Reaction time (RT) across ages groups from pre- to post-error trials.

Age Group	PreFA1	FA	PoFA1	PoFA2
Young	372.40(55.17)	380.43(58.87)	530.57(200.13)	498.04(153.97)
Middle	363.93(53.56)	406.28(154.81)	433.14(165.31)	451(113.13)
Older	479.29(84.37)	489.58(109.89)	533.48(117.31)	529.11(96.26)

Notes: RTs calculated for error NoGo trials (FA), pre-error Go trials (PreFA), and first and second post-error Go trials (PoFA1 and PoFA2). Mean (SD).

To test the effects of RT across age groups as a function of trial order, a linear mixed-effects modelling (LME) was used. Age_group (YA, MA, OA) and trial_order (PreFA_1, FA, PoFA_1, PoFA_2) were used as fixed factors, subjects were used as a random factor, and RT was used the dependent variable. Post hoc β coefficient tests were run using the Satterthwaite correction. The model revealed significant main effects for both age_group ($\mathrm{F}_{(2,299)} = 31.45, \mathrm{p} = 5.16\,\mathrm{x10}^{-13}$), and trial_order ($\mathrm{F}_{(3,897)} = 55.77, \mathrm{p} = 4.66\,\mathrm{x10}^{-33}$), and a significant interactions between the two ($\mathrm{F}_{(6,897)} = 4.07, \mathrm{p} = 4.07\,\mathrm{x10}^{-07}$). Post hoc analyses revealed that the MA group had quicker overall RTs compared to the YA group ($\mathrm{F}_{(1,299)} = 4.71, \mathrm{p} = 0.03$), while RTs were significantly slower in the OA group compared to both the YA ($\mathrm{F}_{(1,299)} = 15.14, \mathrm{p} = 0.0001$) and MA ($\mathrm{F}_{(1,299)} = 62.31, \mathrm{p} = 5.63\,\mathrm{x10}^{-14}$). Next, we explored the effects of trial order, PoFA_1 and PoFA_2 trials had significantly longer RTs than FA trials ($\mathrm{F}_{(1,903)} = 40.81, \mathrm{p} = 2.60\,\mathrm{x10}^{-10}$; $\mathrm{F}_{(1,903)} = 47.24, \mathrm{p} = 1.17\,\mathrm{x10}^{-11}$, respectively), while RTs in PreFA_1 trials were significantly quicker than FA trials ($\mathrm{F}_{(1,903)} = 11.48, \mathrm{p} < 0.0001$). There was no significant difference between post error trial groupings, however PreFA_1 trials had significantly quicker RTs than both post-FA trial groups ($\mathrm{F}_{(1,903)} = 96.42, \mathrm{p} = 1.08\,\mathrm{x10}^{-21}$; $\mathrm{F}_{(1,903)} = 106.16, \mathrm{p} = 1.29\,\mathrm{x10}^{-23}$, respectively). These results show clear effects for PES across all subjects irrespective of age and study. OA subjects had consistently slower RTs in the FA trials compared to both YA and MA of note here in PoFA1 ($\beta = 85.74,\ \mathrm{SE} = 13.47,\ \mathrm{p} = 2.78\,\mathrm{x10}^{-10}, \mathrm{CI}[59.31, 112,16]$; $\beta = 424.31,\ \mathrm{SE} = 5.97,\ \mathrm{p} < 0.0001, \mathrm{CI}[412,61, 436,02]$, respectively). While YA subjects had longer RTs in PoFA1 trials compared to FA trials than did MA group ($\beta = 122.02,\ \mathrm{SE} = 17.44,\ \mathrm{p} = 4.32\,\mathrm{x10}^{-12}, \mathrm{CI}[87.81, 156,23]$).

Changes in grand averaged ERPs across age groups as a function of post-error Go trials (PoFA1, PoFA2, PoFA3, PoFA4) was tested, Figure 7A shows the results for the MA group (for brevity we do not show the results for the Ya and OA groups). To test for significant differences in correct Go trial ERPs across post error trials, a mass multivariate permutation test across channels and time was computed. here only on the results for channel CPz, and likewise not all contrasts are reported but the focus is on the central findings. There was a significant main effect of age_group ($F_{(1,1205)} = 11.75, p = 8.84\,\mathrm{x10}^{-06}, BF_{10} = 1.19\,\mathrm{x10}^{11}$), and a main effect of post-error correct Go trial ERPs ($F_{(1,1205)} = 7.15, p = 9.21\,\mathrm{x10}^{-05}, BF_{10} = 1.34\,\mathrm{x10}^{08}$) and a significant interaction (age_group * trl_order) effect ($F_{(1,1196)} = 3.61, p = 0.002, BF_{10} = 2.91\,\mathrm{x10}^{06}$). Post hoc analyses of the N2 ERP revealed that there was no significant difference between YA and MA ($p = 0.88, BF_{10} = 0.09$). There was a significant difference between YA and OA and MA and OA ($F_{(1,299)} = 16.42,\ p = 6.48\,\mathrm{x10}^{-05}, BF_{10} = 184.35$; $F_{(1,299)} = 18.61,\ p = 2.21\,\mathrm{x10}^{-05}, BF_{10} = 520.27$, respectively). There was a significant difference between MA

vs OA and MA vs YA between PoFA1 and PoFA2 trials $\left(F_{(4,1196)} = 6.92,\ p = 0.009, BF_{10} = 7.33;\ F_{(4,1196)} = 4.83,\ p = 0.02, BF_{10} = 9.747, \text{respectively}\right)$, and no significant difference between YA and OA between PoFA1 and PoFA2. These result show that grand averaged N2 ERPs were not significantly different between the YA and MA across all post-error correct trials but both groups were significantly different from the OA. However, when considering post error action control across trial order, YA and OA participants seemed to produce comparable ERPs, and both groups were significantly different to the MA group.

Group averaged ERPs in post-error correct Go-Hit trials (PoFA1, PoFA2, PoFA3, PoFA4) are illustrated in Figure. 7. To test for significant differences in correct Go-Hit N2 amplitude across subsequent post-error trials, we computed a channel-time cluster permutation LME model testing the relationship between PES and post-FA N2 amplitude of Go-Hit trials ($LME = \widehat{PES}_{\_RT\_ratio} \sim 1 + N2\_Amp_{channel} + (1|Subjects\_ID)$). Specifically, here we focus on channel CPz and found that PoFA1 trial was significantly different from PoFA2, PoFA3 and PoFA4 trials group ($\beta = 0.47,\ SE = 0.24,\ p < 0.05, CI[0.001, 0{,}81]$; $\beta = 0.91,\ SE = 0.86,\ p < 0.001, CI[0.38, 1.33]$; $\beta = 1.78,\ SE = 1.17,\ p = 1.53\ \text{x}10^{-06}, CI[0.71, 1{,}65]$). Similar analyses focusing on P3 amplitude changes as a function of post error trials reveal that PoFA1 trial was not significantly different from PoFA2 ($p = 0.78$), however, PoFA1 was significantly different from PoFA3 and PoFA4 trials group ($\beta = 0.68,\ SE = 0.31,\ p < 0.05, CI[0.08, 1{,}28]$; $\beta = 1.51,\ SE = 0.31,\ p < 1.09\ \text{x}10^{-06}, CI[0.91, 2.11]$). Not all effects are reported here but in general all post error correct Go trials were significantly different from each other ($F_{(3,668)} = 8.73, p = 1.11\ \text{x}10^{-05}$). Our data shows that the N2 and P3 ERP amplitudes changed as a function of post-FA trial order. The morphology of the ERPs would suggest that after an error there is a consistent return to baseline levels. Of note the current results show that post-error slowing was significantly predicted by the size of the preceding ERN.

Finally, we tested the relationship between response slowing properties and both behavioral performance and electrophysiological measures using a robust regression analysis (see Methods). Response slowing is quantified by the ratio between RTs for the post- and pre-NoGo trials (post : pre). Scores greater than 1 represent slowing. Figure 7B illustrates that across all age groups almost all RT ratios for the PoFA2 trials are greater than 1 (post-error slowing PES), and negatively correlated with commission error rates). Specifically, we regressed N2 amplitudes and RTs performance, for brevity we do not report all β coefficients results. Specifically, N2 for the PoFA2 trial was negatively correlated with the RT ratio for the PoFA2 trial across all age groups at CPz ($\beta = 0.47,\ SE = 0.24,\ p < 0.05, CI[0.001, 0{,}81]$; $\beta = 0.91,\ SE = 0.86,\ p < 0.001, CI[0.38, 1.33]$; $\beta = 1.78,\ SE = 1.17,\ p = 1.53\ \text{x}10^{-06}, CI[0.71, 1{,}65]$).

Figure 7E shows the topographical distribution of these β coefficients results, and we can see a clear centro-parietal effect.

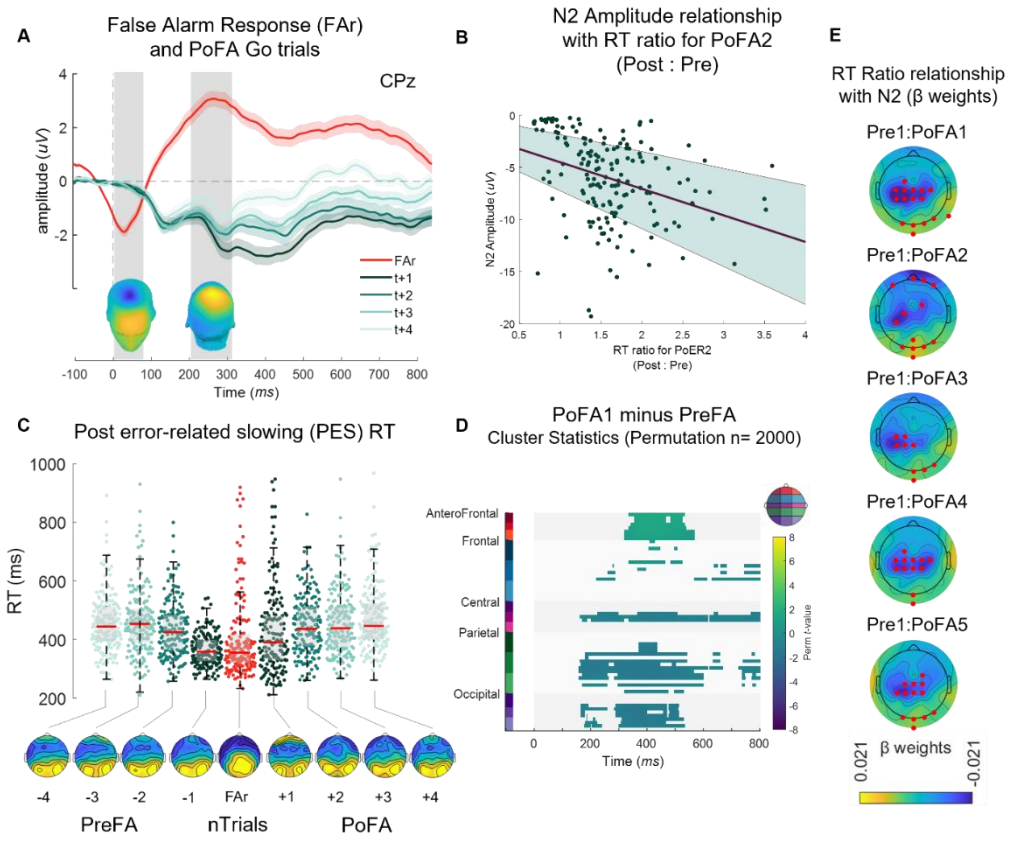

Figure 7 ERN and PES effects. (A) Red line indicates ERN (Response-locked False alarm trials, FAr) and systematic dark to light green, Hit-Go timelocked trials following Far trials, ERPs show +n trials colour coded according to trial distance from error. Shaded Bars demarcate latencies of topographical plot averages. (B) Robust Pearson's correlation between N2 amplitude with RT ratio (PES) for Post-FA t+2 trials (PoFA2). Shaded areas show *CI* [0.001,0,81], single dots represent subjects. (C) PES RT for pre-FA Hit, FA, and post-FA trials Hit trials, single dots are subjects. Box plots (median ± SEM). Topographical plots show averaged data over N2 latencies for the corresponding time-locked trials. (D) Channel-time cluster plot showing main effect of PoFA1 and PreFA trials (only significant data are shown demarcated by colour; *Nperm* = 5000; $p < 0.05$). **(E)** LME beta-wights relationship between PES RT and PoFAn trials across all channels (*Nperm* = 5000, red dots show $p < 0.05$).

6.6 Phase synchrony across trials (ITPC)

Phase synchrony across trials (ITPC)

We used inter-trial phase clustering (ITPC, also referred to as inter-trial phase coherence or phase-locking value (PLV)) as metric to quantify if the distribution of phase angles at each time-frequency-electrode point across trials is nonuniformly distributed in polar space. Trial count influences ITPC. Because ITPC cannot be below zero, noise and sampling errors are more

likely to increase rather than decrease, particularly in few trials. However, in the current analyses we had >60,000 trials in each condition. First we combined data across studies, to determine the overall strength of spatio-temporal phase synchrony across cortical region ROI electrodes (covering frontal, central and temporal-parietal) at a time-window of 0-200 and two frequency bands (delta and theta), and was analysed statistically using a LME model (Conditions (Beh) × ROI × Time-window (Lat) × Frequency-band (Freq)) with these as fixed factors and subjects as random factors, participant age was used as a nuisance regressor. The results are reported in Table 6 and shows there was a significant main effect across all factors and significant interactions between all factors (see Table 6, for details). The results suggest that across our predictors there was a significant difference between Go and NoGo trials. There was a significant interaction for both delta and theta frequency bands across trial conditions with all other factors, and a significant trial condition by laterality by time-window interactions, suggesting differences between Go and NoGo conditions with respect to time interval and scalp distribution of inter-trial synchrony. Furthermore, there was a significant main effect of time-window which is reflected by the increase in ITPC in the post-stimulus intervals compared to the pre-stimulus time-window (-100-0 ms), also indicated by post hoc *t*-tests ($p<0.001$). At both frequencies, ITPC was higher in NoGo trials frontally, and in Go trials parietally. The strongest ITPC differences between Go and NoGo trials were found at the delta frequency: ITPC was higher in Go trials as compared with NoGo trials in the first-time interval after stimulus onset (0–300 ms), especially centro-parietal, whereas in the second time interval ITPC was higher in NoGo trials, especially at frontal and central sites ($p<0.01$, Satterthwaite correction). Figure 8A shows time-frequency plots of the ITPC averaged across subjects separated into the three age groups (YA, MA, OA), plots are shown for FCz channel. Across all age groups we can see significantly stronger ITPC for the NoGo (Cr) trials compared top the Go (Hit) trials; ($cluster\ statistic = 14892.48,\ P = 0.0125$, $cluster\ statistic = 14892.48,\ P = 0.0125$, $cluster\ statistic = 14892.48,\ P = 0.0125$).

Next, we tested the effect on trial type effect (Go (Hits) and NoGo (Cr)) on the phase-angle distribution during an early time-window (0 100 ms) of interest at channel FCz. We contrasted the angle distributions between conditions using a Watson-Williams test on single-trial ERPs filtered in the delta band (1-3 Hz). Figure 8B shows the effect plotted on unit circles (polar plots). These analyses revealed there was no significant difference in phase angle in the YA group ($p = 0.064$), but there was a significant difference for both the MA ($F_{(1,335)} = 97.83, p = 0.001$) and OA ($F_{(1171)} = 12.54, p = 0.001$). Figure 8B also shows the topographic level of the effect (significant channels marked in green), during the time-window of interest, and the bottom panel show the phase variance between the conditions. These analyses revealed one negative cluster in the right occipital-parietal are for the YA participants, there was a significant positive fronto-

central cluster for the MA groups, and finally two positive cluster for the OA participants, one fronto-central and one right occipital-parietal cluster.

Next, we tested the for a main effect of age group and the phase of the response inhibition effect (the EEG phase Go – NoGo trials) using a cluster-based permutation test in the theta frequency range (4-8 Hz). Figure 8C left panel shows these results, we can see a clear difference in response inhibition effect starting in the prestimulus window and extending to the early post stimulus window. Significant positive cluster can be seen in frontal, parietal, and some central channels $cluster\ statistic = 849.01,\ P = 0.001$).
Finally, we wanted to test the relationship between the phase of the response inhibition effect in channel FCz across age (age was defined as a continuous variable but is colour coded into the three age groups, see figure legend). Using a robust Spearman's correlation analysis with bootstrap resampling (Pernet, Wilcox, & Rousselet, 2013) the results show a significant positive relationship ($r_s = 0.31,\ p = 4.33\,\mathrm{x}10^{-04}, 95\%\ CI\ [0.09 - 0.30]$).

Table 6. Linear-mixed effects model results (F and *p* values) for ITPC estimates across weights Condition × Beh × ROI × Lat × Freq.

Factors	F value	*p* value
Intercept*	1308.500	1.11E-208
Freq	19.232	1.19E-05
Beh	30.007	4.58E-08
Lat	408.140	2.46E-86
ROI	76.393	2.92E-33
Freq*Beh	3.279	7.03E-02
Freq*Lat	54.293	2.10E-13
Beh*Lat	0.116	7.33E-01
Freq*ROI	2.341	9.63E-02
Freq*Beh	2.433	8.79E-02
Lat*ROI	25.735	7.90E-12
Freq*Beh*Lat	18.420	1.82E-05
Freq*Beh*ROI	2.296	1.01E-01
Freq*Lat*ROI	11.515	1.03E-05
Beh*Lat*ROI	10.995	1.73E-05
Freq*Beh*Lat*ROI	6.929	9.91E-04

Notes: ITPC = Inter-trial phase clustering; Beh = Go (Hit) and NoGo (Cr) trials; Freq = frequency (delta 2-4 Hz and theta 4-8 Hz); Lat = latency of time-window of interest (early 0-300 ms and late 300 - 600 ms); ROI = region of interest (Central, Left, Right)

Interregional functional connectivity

We assessed functional connectivity between EEG electrodes to investigate the structure of the response inhibition network in delta and theta frequency bands. Based on the ITPC results previously presented, here we focused on two different time and frequency windows. Specifically, an early (0-300 ms) and late (300-600 ms) in the delta (2-4 Hz) and theta (4-8 Hz) frequency bands. Cluster-correction was used at a significance threshold of p = 0.05/2 = 0.025. The extent of spectral coherence between every pair of electrodes was calculated using

debiased weighted Phase Lag Index (dwPLI (Vinck et al., 2011)) metric. dwPLI is a sensitive measure of true connectivity between cortical regions that has been shown to be robust against the influence of volume conduction, uncorrelated noise, and inter-subject variations in sample size. First, we ran a full brain connectivity analysis, then we performed a data reduction where we restricted the analyses of dwPLI to a set of 10 electrode (AFz, FC5, FC6, FCz, C3, C4, CPz, PO7, PO9, Oz) which in turn formed 18 electrode connection pairs. These are most representative of the major scalp coverage and form part of response inhibition network and define the major-regional connections.

In line with the previous ITPC analysis, dwPLI for all these connections was determined by the overall strength of spatio-temporal phase synchrony across cortical region ROI electrodes (covering frontal, central and temporal-parietal) in two time-windows (early: 0-200; late; 200-600 ms) and two frequency bands (delta and theta), and was analysed statistically using a LME model (Conditions (Beh) × ROI × Time-window (Lat) × Frequency-band (Freq)) with these as fixed factors and subjects as random factors, participant age was used as a nuisance regressor. Specifically, we took the mean absolute value of the dwPLI, which is an index of phase synchrony strength and is bidirectional. These results are reported in Table 6 and indicate the significant main effects of all four predictors and the significant interactions between these estimates. There was a significant main effect for Condition (Beh: Cr (Go) and onFA), Frequency (Freq), Latency (Lat), and ROI. There were significant interactions across all factors, there was a significant interaction of Freq*Beh*Lat*ROI.

Figure 9 shows the average dwPLI values for each of these 18 electrode connection pairs by time-window, frequency band, and condition. As illustrated, phase connectivity was stronger for Cr (NoGo) compared to onFA trials. There was a significantly stronger functional network connectivity in the late theta frequency band window compared to the early delta frequency band window in the Cr trials. These results also show a clear stronger right-lateralized connectivity during trials where subjects were able to accurately inhibit responses. While this network was significantly weaker for the onFA trials. Although, early theta frequency band window showed the stronger functional network connections for onFA trials, which appears to be more right-lateralized.

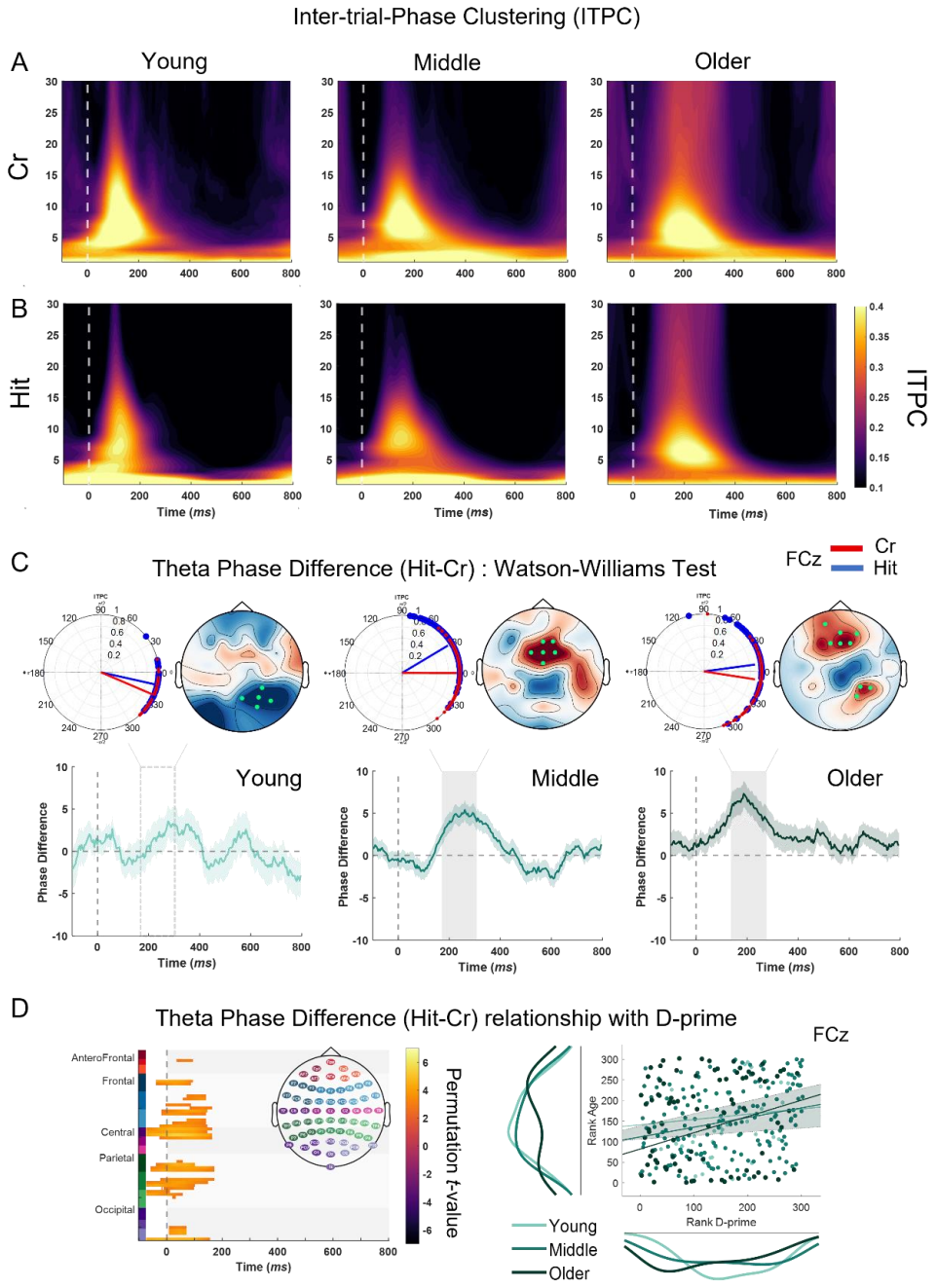

Figure 8. Inter-trial-phase clustering. Grand-averaged stimulus-locked time-frequency plots of inter-trial phase clustering (ITPC) for **A.** Go (upper row) and **B.** NoGo (bottom row) trials (conditions) plotting for FCz channel. The min/max range in the case of the time-frequency diagrams corresponds to 0.12/0.48. **C.** Phase distribution difference (Watson–William's test across trials) at the topographical level between Go-Hit (blue) and NoGo-Cr (red) trials in theta (4–8 Hz) band. Bold green dots highlight the cluster of sensors that reach the $P < 0.05$ significance threshold and survived correction for multiple comparisons. The following analyses of theta phase are computed on the circular average of phase signals extracted from FCz channel. Unit circles (polar plots) show the distribution of theta-phase angles across trials in the time window of interest. Phase-angle distributions significantly differ between Go-Hit (blue) and NoGo-Cr (red) trials (Watson–William's test; $P < 10-4$). Bottom panel shows, a linear conversion of the distance between phase angles. Shaded area demarcates SEM. Grey bars indicate temporal regions that are significantly difference between conditions using a cluster-based permutation test (Nperm = 2000, $p < 0.05$). **D.** Left panel, relationship between response inhiation effect (Hit-Cr) EEG phase and behavioral performance (D-prime) across channel and time in the theta frequency range. Robust Pearson's correlations with density curves (bootstrap permutation test $p < 0.05$, confidence interval 95%). Left panel shows this effect specifically in channel FCz. All data are colour coded according to group type. Left panel, shows the same relationship.

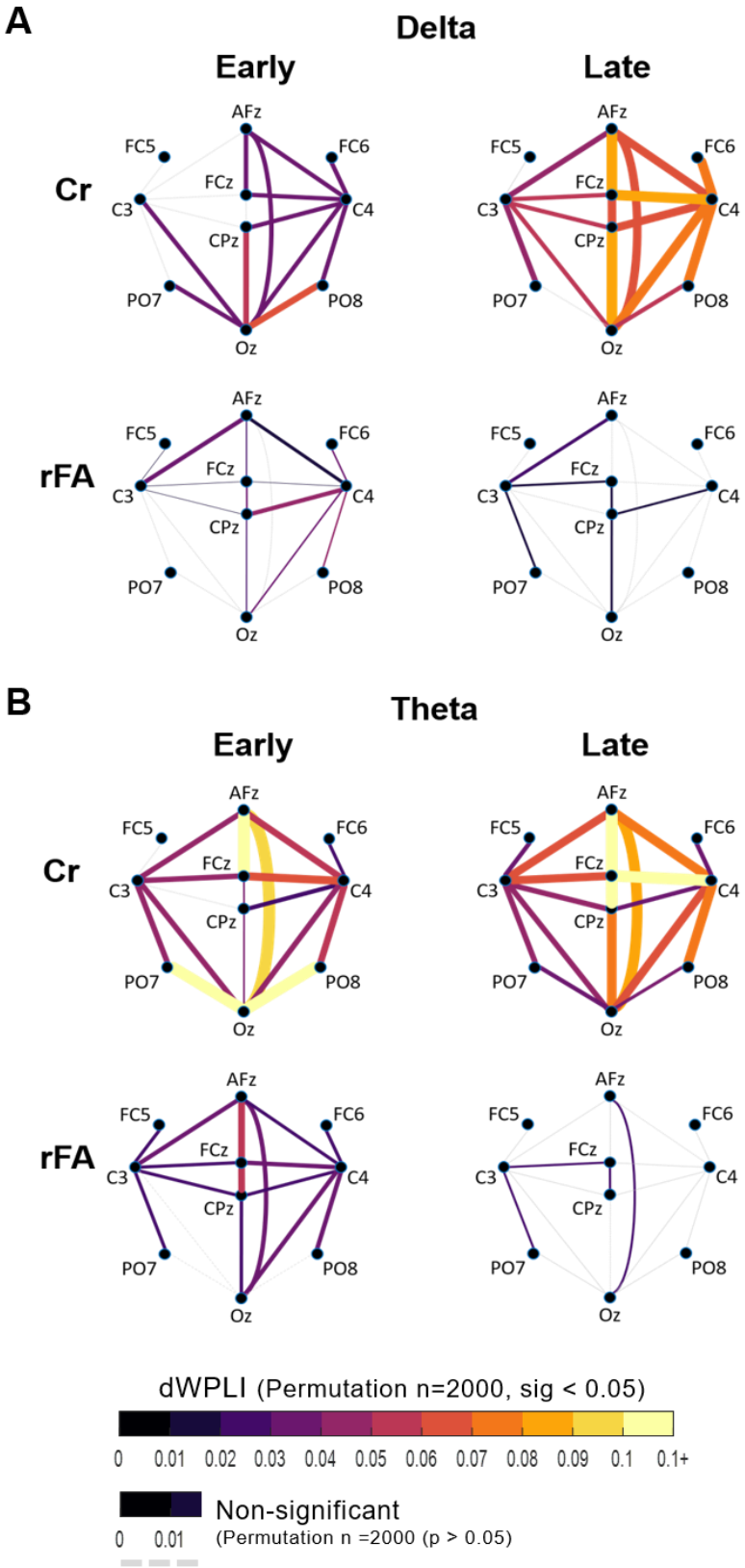

Figure 9. Grand average stimulus-locked functional connectivity diagrams of dwPLI in the Go (Cr) and onFA conditions. Electrode maps show dwPLI values for each electrode pair averaged within the two-consecutive time-

windows (Early and Late) after stimulus onset, separately for delta and theta frequency bands. dwPLI between the electrodes is represented through connections between the electrodes, which are coded with color to specify connection strength (connection strength is the absolute value of the dwPLI between two electrode pairs) from black (low dwPLI) to yellow (high dwPLI). Specifically, the thickness of the edges are proportional to the dwPLI weight.

7 Discussion

The aim of the current paper was to introduce a data repository of 302 healthy subjects performing small variants of a Go/NoGo response inhibition task. This provides some initial preliminary insight into comparisons across datasets and permits replication of some of the main behavioral and electrophysiological results presented in the response inhibition literature. One main aim of the current paper is to demonstrate the efficacy of the high-density EEG dataset and its' potential use to explore new avenues of research in response inhibition using neurobehavioral measures. The second aim pertains to that of open science. Currently research is rapidly moving towards sharing and making freely available cognitive neuroimaging data repositories. This has largely been the catalyst in the steep increase in the number of participants that are included in any given study. This surge in "N" has provided superior statistical power and reduced vulnerability to spurious effects and presents opportunities to enhance reproducibility in neuroimaging research. For example, the current large dataset affords the opportunity to examine, more robustly, previously known underpowered analyses within this field (e.g., event-related negativity (ERN) or post-error related slowing (PES)). The large number of trials enables new questions to be asked that cannot be answered with single datasets. This repository may be used to obtain regression-based methods of both EEG electrophysiological and behavioral measures, to study spectral analysis, single-trial based measures and to study functional connectivity at the scalp level.

Increasingly research has focused on impairments to response inhibition resulting from the healthy aging process. Here we show comparisons across a wide range of ages from typical maturation in young teens to healthy older adults. For the purposes of the current study, to investigate effects of age, the data were pooled across studies and grouped into three age groups (YA, MA, OA). It is important to note here that young adulthood is usually studied within a wide age range (from 18 to 40 years of age) making it rather difficult to acquire an accurate and comprehensive description of response inhibition development. This is made additionally complicated because maturation changes can be quite protracted during emerging adult years. Nonetheless, the current data repository offers an opportunity to further characterize the neural profile underlying response inhibition ranging from young to older adults. Our results provide an important insight into the changes of behavioral and brain-based indices of response inhibition across age.

Behavioural response inhibition performance across age

First, we assessed behavioral performance across the studies and then collapsed across these according to three age groups. Multiple studies report a general decline in cognitive processing among the elderly (Friedman, Simpson, & Hamberger, 1993; McDowd, Oseas-Kreger, & Filion, 1995), however the average age of our oldest group could still be classified as late-MA aged adults and no decline in our behavioral measures was observed. No significant increase in RT with increasing age was observed, and no significant relationship as a function of age was found across all behavioral measures. Interestingly, performance with respect to commission errors was also not influenced by age, which is consistent with other studies showing heterogeneous results for Go/NoGo tasks (Grandjean & Collette, 2011; Hu, Chao, Winkler, & Li, 2012; Langenecker & Nielson, 2003; Nielson, Langenecker, & Garavan, 2002; Vallesi, 2011). Behavioral performance in OA adults is characterized by a trading of speed for maintenance of accuracy. In line with this suggestion, the rate of omission correlates positively with age (Christakou et al., 2009). A non-significant finding could be attributed to the age range with which we chose to split the groups. Age-dependent changes in behavioral correlates of response inhibition are more clearly expressed before young adulthood, e.g. MA school age children (Johnstone et al., 2007), although the current findings suggest that within the Young cohort defined here demonstrate stable performance resembling adult levels. Previous work suggests that the ability to inhibit prepotent responses becomes faster as age increases during childhood and shows only a slight slowing during maturation in childhood, while response execution shows improvement during childhood and a marked slowing throughout adulthood, suggesting different developmental time courses for these processes (Band et al., 2000; Falkenstein et al., 2002).

Many developmental studies have shown that cognitive control becomes more efficient (i.e., faster, and more accurate) with development (Keating & Bobbitt, 1978), not reaching full maturity until after age 12 (Passler, Isaac, & Hynd, 1985). Considering our average age in the young group was 18 years old, this may explain why the presented results were largely non-significant across the groups. Moreover, parametrically increasing the number of Go trials preceding a NoGo trial has been shown to increase the task difficulty. Specifically, as the number of preceding consecutive Go trials increases, people show a greater proportion of FAs to NoGo trials (Durston, Thomas, Worden, Yang, & Casey, 2002) and longer RTs to Go trials (Liston et al., 2006). This manipulation provides a particularly sensitive probe of developmental changes in attentional control. Across the current included studies in our repository on average NoGo trial proportions were about 14%, and therefore may not be best placed to tease apart these effects.

Finally, the results show that behavioral performance was not affected by type of EEG lab (standard or MoBI) nor did ISI or stimulus duration have an effect on these measures. Previous studies have reported different ISI's (Lee et al., 2009; Oerlemans et al., 2013; Zamorano et al., 2014) and these have been defined in various ways (Kuiper, Verhoeven, & Geurts, 2016; Metin, Roeyers, Wiersema, van der Meere, & Sonuga-Barke, 2012). Further manipulations across studies include "stimulus-type" which could consist of pictures that have a categorized emotional valence attributed to them (e.g., IAPS) and these can further be grouped into scenes of inanimate objects or faces conveying emotion, or these could be simple shapes or text. The use of emotional stimuli, for example, could lead to reduced performance of people with ASD, as ASD is associated with emotion processing deficit (Cassidy, Mitchell, Chapman, & Ropar, 2015; Philip et al., 2010). These differences in ISI and "stimulus-type" could be part of the unknown factors that influence inhibitory control in people with ASD but might not have the same effect on inhibitory control in healthy participants.

Neurophysiology of response inhibition

Research suggests that both N2 and P3 components are indices of motor inhibition, specifically the response control function that is engaged on the NoGo trials (Huster et al., 2013). Previous work has shown that N2 amplitude and latency decreases with increasing age (Jonkman, 2006), which suggests a more efficient engagement of cognitive control with age. Our results show that the N2 component was significantly greater in the NoGo trials for both MA and OA aged groups. However, this was more pronounced in the OA group, while the opposite was found in the YA group. The N2 in the MA groups was sharper in morphology and had shorter latency compared to the OA group. We found this effect to be maximal at central or posterior locations rather than more frontal. We found subtle yet significantly enhanced N2 amplitudes in the MA and OA aged groups. Specifically, this was enhanced in the OA group. While N2 amplitudes had a deflection towards negativity but remained positive in the YA group. Interestingly, both the OA and YA groups had later N2 amplitude timings compared to the MA group. An enhanced N2 seen in NoGo-Cr trials compared to Go-Hit trials is consistent with the literature, although exactly what this underlying neural response captures is still debated. However, it has been previously argued that the N2 is to be considered as less reliable marker of response inhibition than the P3 (Kropotov et al., 2011; Randall & Smith, 2011; Smith, Johnstone, & Barry, 2007). Furthermore, frontal P3 amplitude has been associated with increased response inhibition and is similarly related to attentional demands and novelty processing (Wessel, 2018; Wessel & Aron, 2015) Our data provide support for a significant NoGo-N2 across our various analyses corroborate other visual Go/NoGo tasks (Falkenstein et

al., 1999; Jodo & Kayama, 1992).

We found a significant modulation of P3 across the age groups, the P3 amplitude decreased in size as a function of participant age. However, in contrast to some previous findings, we did not see a systematic relationship between P3 decrease and N2 decrease with age (Kropotov, Ponomarev, Tereshchenko, Müller, & Jäncke, 2016; Kropotov et al., 2011). Although these studies cued participants which could explain variations in ERP morphology. Our data shows, the P3-activation declines in amplitude and latency with age. This could correspond to the hypothesis of an inhibition deficit in the elderly (Lustig, Hasher, & Zacks, 2007).

Error-related negativity (ERN/Ne) in Pre- and Post-Error trials and relationship with post-error slowing (PES/Pe)

The ERN is an early component associated with error detection and performance monitoring after error commission (Danielmeier & Ullsperger, 2011; Ullsperger, Fischer, Nigbur, & Endrass, 2014; Wessel, 2012). One important consideration when measuring ERN is to ensure there is sufficient number of error trials with which to accurately measure error-related componentry. In the current study we took advantage of our large participant sample and large trial numbers to investigate the neural processes associated with post-error adjustments. Our findings revealed that error trials yielded both ERN and Pe evoked components, consistent with findings in the literature (Botvinick, Braver, Barch, Carter, & Cohen, 2001; Coles, Scheffers, & Fournier, 1995; Debener et al., 2005; Gehring, Goss, Coles, Meyer, & Donchin, 1993; Taylor et al., 2007). All studies included in the current reposit yielded negative potentials corresponding to ERN/Ne and positive potentials for Pe, indicating that on average participants engaged with error monitoring.

Post-error slowing is the observed prolonged RT in trials subsequent to an error compared to RTs in pre-error (FA) trials (Rabbitt, 1966). In the current study however, participants exhibited a delayed post-error recovery from rash response patterns as exhibited on PoFA1 trial, as demonstrated by their faster responses compared with those in the PreFA trials. Few studies have reported similar post-error recovery (King, Korb, von Cramon, & Ullsperger, 2010; Soshi et al., 2015) while other report similar post-error speeding but where errors were at 75% frequency (Notebaert et al., 2009). While others report no evidence of PES under different study conditions (Fiehler, Ullsperger, & Von Cramon, 2005; Ullsperger & Falkenstein, 2004). On the contrary two previous experiment only observed PES in condition where errors were infrequent (Notebaert et al., 2009; núñez Castellar, Kühn, Fias, & Notebaert, 2010). To this end, it remains unclear under which conditions PES can be observed, and what the underlying neural mechanisms are (Danielmeier & Ullsperger, 2011).

It is clear (see, Figure 7) that participant responses gradually became faster until the error occurred and then significantly slowed after the error (as observed in PoER trials n+; 1,2,3,4). This finding is consistent with the hypothesis that participants adjust their speed in response to errors (Laming, 1979; Rabbitt & Rodgers, 1977) or conflict (Botvinick et al., 2001). Our results show that post-error slowing was significantly predicted by the size of the preceding ERN. However, the literature on the relationship between error-ERPs and post-error RT adjustments are equivocal. There are some reports of such correlations (Debener et al., 2005; Gehring et al., 1993; Nieuwenhuis, Ridderinkhof, Blom, Band, & Kok, 2001; Rodríguez-Fornells, Kurzbuch, & Münte, 2002), while others report no or contradictory evidence (Gehring & Fencsik, 2001; Hajcak, McDonald, & Simons, 2003; núñez Castellar et al., 2010). Understanding the variables that influences the ERN and how it in turn impacts behavior is of particular relevance. More specifically, the ERN presents a potential readout of the influence of affective information on cognitive monitoring of behavior, and thus understanding gained from analysis of this dataset has potential implications for clinical research relates to the application of ERN to index affective processing is increasingly becoming of great importance and most specifically clinically meaningful, as the ability to modulate behavior in line with one's own motives and the salience associated with different outcomes is fundamental to goal-directed behavior (Pailing & Segalowitz, 2004).

In the current study, the large participant cohort enabled investigation of event-related negativity (ERN) and post-error slowing (PES) effects on large trials numbers across conditions (n = 37584 trials on average per condition). The literature is mixed on the presence of such a relationship; however, this may be due to the typically small numbers of error trials in Go-NoGo student, leading to a noisy signal and a lack of statistical power. Here, where we are able to overcome this issue due to large amounts of data and ensuing statistical power, our findings are consistent with studies that have found that larger ERN amplitudes are associated with increased PES (Gehring et al., 1993).

A significant negative relationship between N2 amplitude from both the PoER1 and PoER2 trials with PES was found, suggesting that greater N2 activity is associated with greater post-error recovery. Previous literature, suggests that N2 occurring during PoER1 and PoER2 trials is likely to reflect cognitive control after errors (Folstein & Van Petten, 2008; Rietdijk, Franken, & Thurik, 2014). Change et al. (2014), further demonstrated that the N2 enhancement was observed for PES. This N2 modulation may contribute to resetting the predisposition to respond with a button press, as represented by the negative correlation between pMFC and motor areas (Danielmeier et al., 2011) or enhanced activation of the ventrolateral PFC connected with the SMA (Li et al., 2008b; Ide and Li, 2011), or may reflect monitoring the conflict between Go and

NoGo response selections (Botvinick et al., 2001).

The decline of inhibitory control in OA adults has been shown for several inhibitory tasks including the Simon task or the Stop-signal tasks (Andrés, Guerrini, Phillips, & Perfect, 2008; Hu et al., 2012; Maylor, Birak, & Schlaghecken, 2011; Van der Lubbe & Verleger, 2002; West & Alain, 2000; Williams et al., 1999). However, studies using Go/NoGo tasks often report either impaired or equal performance depending on the complexity of the task (De Sanctis et al., 2014; De Sanctis et al., 2020; Grandjean & Collette, 2011; Rush, Barch, & Braver, 2006; Vallesi & Stuss, 2010). The Go/NoGo task is the least complex task, as it offers only two conditions (Go and NoGo), and thus it is not surprising that we did not find this relationship in the current dataset. This is especially the case given that our older adults were younger on average than those typically included in such a group.

Finally, a significant systematic modulation in post-error Go trial ERPs. Specifically, in the MA aged group the results show that with increasing trials post stimulus (PoER +1,+2,+3,+4) ERP amplitudes for both N2 and P3 are modulated as a function of trial distance from error trial. Our results suggest that there is a systematic increase in top-down and inhibitory control in the preparation of the trials following error commission. Others have found that this effect is localised to premotor areas (Perri et al., 2016). We observed a significant negative relationship between response slowing as quantified by the ratio of reaction times (RTs) for between the post- and pre-error Go trials (post:pre) or otherwise referred to as Post-Error-Slowing (PES). Across all ages there was a significant slowing in RT from pre-post error trials that correlated with the negative deflection of the N2 component. In other words, N2 increases with the degree of conflict between two response units, which delays motor activation and prolongs RT (Yeung, Botvinick, & Cohen, 2004), consistent with our finding that N2 is larger in amplitude during PES than non-PES trials. We further found that this effect was significant over fronto-central electrodes. Studies using source space analyses showed that anterior N2 is likely to originate from the medial frontal cortex including the anterior cingulate cortex (Botvinick et al., 2001; Yeung et al., 2004). And the current data repository offers a unique opportunity to explore these effects further in source space. These findings suggest that N2 during PoER1 and PoER2 trials are a modulated as a function of cognitive control and form a monitoring mechanism which contributes to PES (Chang, Chen, Li, & Li, 2014). The findings corroborate earlier studies showing that the amplitude of ERN increases with the extent of PES (Debener et al., 2005; Gehring et al., 1993; Wessel & Ullsperger, 2011; West & Travers, 2008), in support of the conflict monitoring hypothesis (Yeung et al., 2004). There was also significant positive correlation between error-related positivity (Pe) and ERN. However, studies have also reported results inconsistent with the conflict monitoring hypothesis. For instance, the amplitude of ERN did not

predict the magnitude of PES (Hajcak et al., 2003; Nieuwenhuis et al., 2001).

Functional spatial synchrony between ROI nodes as indicated by dwPLI

Finally, task-related functional changes in the synchrony of neural oscillations was investigated by means of phase synchronisation (ITPC) within and between interregional (dwPLI) electrodes as a function of continuous task performance. Unsurprisingly, both synchronisation measures were systematically increased in the Go (Hit) and NoGo (Cr) conditions as compared with FA (rFA and onFA) trials. Our main findings concerning Hits vs Cr and Cr vs FAs are as follows: (a) both synchronization measures (ITPC and dwPLI) showed strongest effects in the delta frequency band; (b) both measures showed also strong modulations by scalp topography, frequency and time course related to Go/NoGo differences; whereas ITPC in Go trials reach their maxima in the first post-stimulus time interval (0–400 ms), these synchronization measures in NoGo trials showed strongest effect in the second post-stimulus time interval (400–600 ms). Although phase synchronization (especially, measured by ITPC) was in general highest at fronto-central and right lateralized centro-parietal sites, phase synchronization in Hit trials was stronger than in FA trials in the first-time interval at centro-parietal sites, phase synchronization in NoGo trials was stronger than in Go trials in the second time interval at frontal and central sites.

Previous research has shown that phase synchronisation across trials as measured by ITPC (or phase-locking index, PLI) is associated with stronger neural timing induced through stimulus processing and is a possible candidate mechanism of temporal coding used by neural ensembles for stimulus processing and encoding [REF]. While dwPLI is posited as a measure of interactive neural synchronisation or integration of numerous functional areas widely distributed over the brain [REF]. Therefore, a plausible interpretation of our findings suggests that stimulus processing in the Go and NoGo trials as compared to the FA trials produce more synchronous activity at different electrode locations in the response inhibition network and with greater synchronisation patters during trials where participants accurately inhibited responses.

The most general effect concerning both synchronization measures (i.e., ITPC and dwPLI) and both frequency bands (i.e., delta and theta) is related to earlier synchronization in Go as compared with NoGo trials. Interestingly, this fast synchronization in Go trials reaching their maxima in the first-time interval (0–400 ms) remain stable in the second time interval (400–600 ms) at parietal sites showing strongest effect and decreases at frontal and central sites. In NoGo trials, phase synchronization increases continuously through the two post-stimulus intervals at all brain regions (especially frontally) and reach their maxima during the second time interval.

Using dWPLI as an index of inter-regional functional connectivity we reduced all our electrode connections down to a response inhibition ROI network. We found significantly stronger right lateralized connections in the late-time windows for both delta and theta frequency for the Cr(NoGo) trials compared to the rFA trials. A similar but slightly weaker right lateralized functional network was found in the early-time window in Cr(NoGo) compared to rFA trials, however there were significantly stronger connections in the theta frequency ranged compared to delta frequency. Specifically, we found stronger connections between C4-FCz, AFz-FCz in the late time-window, while interestingly we found stronger visual connections Oz-PO8 and Oz-PO7 in the early time-window in theta frequency range compared to delta. Our findings of a right hemisphere dominance in the response inhibition network have been well documented in previous findings (Chikazoe, Konishi, Asari, Jimura, & Miyashita, 2007; Garavan et al., 1999; Konishi, Nakajima, Uchida, Sekihara, & Miyashita, 1998; Zheng, Oka, Bokura, & Yamaguchi, 2008). Specifically, Go/NoGo studies have argued that motor response inhibition is strongly lateralized to the right hemisphere (De Zubicaray, Andrew, Zelaya, Williams, & Dumanoir, 2000; Garavan et al., 1999; Kawashima et al., 1996; Konishi et al., 1998).

Often enhanced oscillatory phase alignment in the delta frequency during cognitive tasks is indicative of attentional task demands (Harmony et al., 1996; McEvoy, Pellouchoud, Smith, & Gevins, 2001). Specifically, recent work has shown a positive relationship between delta phase synchronisation and task performance in young adults while there is a negative relationship in OA adults (Müller, Gruber, Klimesch, & Lindenberger, 2009). In the current study, increased delta phase synchrony can be paralleled to the Go-P3 and the NoGo-P3 components, in terms that the former has been proposed to reflect response-related cognitive processing, while the later has been liked to response inhibition (Bekker, Kenemans, & Verbaten, 2005). Therefore, this low frequency phase synchronisation in Go trials during the first-time interval (0-300 ms) showing centro-parietal brain activity distribution is in line with the premise that attentional load is related to response execution as mentioned previously, while the low frequency phase synchronisation in the NoGo trials is argued to be required to accurately suppress undesirable responses. This assumption is corroborated with previous ERP studies showing a relation between NoGo-P3 and the anteriorization of this component to response inhibition, rather than to conflict monitoring (Fallgatter & Strik, 1999; Pfefferbaum & Ford, 1988; Pfefferbaum, Ford, Weller, & Kopell, 1985; Salisbury, Griggs, Shenton, & McCarley, 2004). Increased frontal theta connectivity in Cr(NoGo) trials could be indicative of a modulation frequency for the frontal N2 component, which is strongly enhanced in the Cr(NoGo) trials and diminished or even absent in rFA or Go trials (Jonkman, Sniedt, & Kemner, 2007; Jonkman, 2006), and we speculate that this reflects a more general process of conflict monitoring, rather than suppression of motor

responses.

Standardization of EEG for multi-site, multi-platform and multi-investigators

One major initial concern in combining multi-site EEG data is the identification and assessment of sources of variability that can impact the EEG outcomes and how to make them comparable or how best to standardize across datasets. EEG data collected from different devices may be different due to external factors not related to neurophysiology but to hardware differences, amplifiers, noise, and other factors. Additionally, factors like the skull thickness, hair, skin conductance, etc. may be the source of other differences in the EEG recordings. Inter-dataset variability in neuroimaging studies and specifically here EEG, can originate from errors or differences in study design (e.g. ISI, stimulus-type, stimulus duration, trial numbers), experimental setup and laboratory conditions (EEG testing booths or MoBi lab), equipment (e.g. EEG cap montage Biosemi setup), data quality control procedures (EinMed and UoR have similar procedures in place) and data preprocessing and analyses (all data we passed through the same processing pipelines and analysed with the same analyses software and procedures). It's important to note that these factors may not be evident in the initial stages of study design and only evident when integrating across multiple datasets.

Due to the longstanding collaboration that exists between the Elbert Einstein College of Medicine and the University of Rochester, data collection procedures across the two sites follow similar guidelines and procedures. This has meant that many unwanted potential extraneous factors have been controlled for, such as hardware and experimental setup. Furthermore, participant instructions were similar across sites. All analyses were carried out in MATLAB (The Mathworks, Inc., Natick, MA, USA). Firstly, raw data files were re-configured into the same file formats and composition. For example those datasets collected from Mobi required additional preprocessing steps as these were collected with Lab Streaming Layer (LSL) data acquisition and control framework of Christian Kothe (Delorme et al., 2011). Freely available functions to convert *.xdf* file format to Matlab *.mat* files which can be found here: https://github.com/xdf-modules/xdf-Matlab (Ojeda, Bigdely-Shamlo, & Makeig, 2014). Furthermore, Biosemi *.bdf* files were converted to *.mat* files using Fiedltrip toolbox. Further preprocessing steps are detailed in the *Methods* section of this paper. All data were processed through a single pipeline created from a combination of custom in-house code and various libraries from toolboxes such as Fiedltrip and EEGLAB. Some modification was needed depending on the experimental setup.

The next procedure that was put into place to ensure consistency across datasets during the preprocessing stage was to use an automatic independent component analysis (ICA) referred

to as ICLabel, which is a pre-trained neural network based on the power spectra and spatial distribution of the ICs (Pion-Tonachini et al., ICLabel: An automated electroencephalographic independent component classifier, dataset, and website, 2019). ICLabel training is performed on a dataset containing over 200,000 ICs from more than 6000 EEG recordings (Pion-Tonachini et al., The ICLabel dataset of electroencephalographic (EEG) independent component (IC) features, 2019).

Next, by means of interpolation, all EEG datasets were reduced to a common electrode space of a 64-channel montage (BioSemi 10/20 layout). We chose a 64-channel layout as this was the lowest channel number across all the datasets. To do this, the neighborhood structure of each dataset was defined, and a weighted-average of nearest-neighbours interpolation was used to systematically reduce channels down to a 64-channel montage for each dataset with headcaps larger than a 64-channel layout. Original montages of each dataset are available in the data repository.

Finally, it is beyond the remit of the current paper but there exist various approaches to quantify or control for these extraneous non-neurophysiological factors affecting EEG recordings, including a random scale factor (normalisation; GSF), using principle component analysis (Hernández et al., 1994), or general procedures using LORETA gaussian smoothing to reduce intersubject variability (Leuchter et al., 1993; Nuwer, 1988). In the former it has been shown that the maximum likelihood estimate of GSF for an individual is the average log power values across all deviation. Correcting across the EEG datasets by this factor may assist in eliminating individual differences making recordings more comparable for statistical purposes.

Data archiving

To enable replication of results, archiving of the outputs of intermediate analyses steps was done. Including the original raw unprocessed file formats from each study. All published datasets are de-identified and are archived and organised according to standards and guidelines following the BIDS format. The results of the present study will be made available at [INSERT WEBISTE].

Conclusions

The amount of openly available shared neuroimaging data has substantially increased over the past decade as the movement towards Open Science grows stronger with each passing year. Several researchers have argued that more rapid scientific discoveries are possible within a culture of shared data (Ascoli, Maraver, Nanda, Polavaram, & Armañanzas, 2017; Ferguson, Nielson, Cragin, Bandrowski, & Martone, 2014; Milham, 2012; Poldrack, 2012; Poldrack &

Gorgolewski, 2014) and that some questions can only be answered with large datasets or meta-analysis. In sum, we present a healthy normative EEG database of participants performing a response inhibition Go/NoGo task. We show both behavioral and neurophysiological correlates associated with motor inhibition, conflict monitoring and post-error action control. We further demonstrate age-related relationships across these cognitive functions. In doing so demonstrate the potential efficacy of the current database and its' possible utility to further investigate brain-behaviour electrophysiology in the inhibitory network.

8 References

Acunzo, D. J., MacKenzie, G., & van Rossum, M. C. (2012). Systematic biases in early ERP and ERF components as a result of high-pass filtering. *Journal of Neuroscience Methods, 209*(1), 212-218.

Albert, J., López-Martín, S., Hinojosa, J. A., & Carretié, L. (2013). Spatiotemporal characterization of response inhibition. *Neuroimage, 76*, 272-281.

Andrés, P., Guerrini, C., Phillips, L. H., & Perfect, T. J. (2008). Differential effects of aging on executive and automatic inhibition. *Developmental neuropsychology, 33*(2), 101-123.

Aron, A. R., Fletcher, P. C., Bullmore, E. T., Sahakian, B. J., & Robbins, T. W. (2003). Stop-signal inhibition disrupted by damage to right inferior frontal gyrus in humans. *Nat Neurosci, 6*(2), 115-116.

Aron, A. R., & Poldrack, R. A. (2005). The cognitive neuroscience of response inhibition: relevance for genetic research in attention-deficit/hyperactivity disorder. *Biological psychiatry, 57*(11), 1285-1292.

Ascoli, G. A., Maraver, P., Nanda, S., Polavaram, S., & Armañanzas, R. (2017). Win–win data sharing in neuroscience. *Nature methods, 14*(2), 112-116.

Band, G. P., Ridderinkhof, K. R., & van der Molen, M. W. (2003). Speed-accuracy modulation in case of conflict: the roles of activation and inhibition. *Psychol Res, 67*(4), 266-279.

Band, G. P., van der Molen, M. W., Overtoom, C. C., & Verbaten, M. N. (2000). The ability to activate and inhibit speeded responses: Separate developmental trends. *Journal of experimental child psychology, 75*(4), 263-290.

Baumeister, S., Hohmann, S., Wolf, I., Plichta, M. M., Rechtsteiner, S., Zangl, M., . . . Meyer-Lindenberg, A. (2014). Sequential inhibitory control processes assessed through simultaneous EEG–fMRI. *Neuroimage, 94*, 349-359.

Bekker, E. M., Kenemans, J. L., & Verbaten, M. N. (2005). Source analysis of the N2 in a cued Go/NoGo task. *Cognitive Brain Research, 22*(2), 221-231.

Blasi, G., Goldberg, T. E., Weickert, T., Das, S., Kohn, P., Zoltick, B., . . . Mattay, V. S. (2006). Brain regions underlying response inhibition and interference monitoring and suppression. *European Journal of Neuroscience, 23*(6), 1658-1664.

Bokura, H., Yamaguchi, S., & Kobayashi, S. (2001). Electrophysiological correlates for response inhibition in a Go/NoGo task. *Clinical neurophysiology, 112*(12), 2224-2232.

Bokura, H., Yamaguchi, S., Matsubara, M., & Kobayashi, S. (2002). *Frontal lobe contribution to response inhibition process—an ERP study and aging effect.* Paper presented at the International Congress Series.

Botvinick, M. M., Braver, T. S., Barch, D. M., Carter, C. S., & Cohen, J. D. (2001). Conflict monitoring and cognitive control. *Psychol Rev, 108*(3), 624.

Button, K. S., Ioannidis, J. P., Mokrysz, C., Nosek, B. A., Flint, J., Robinson, E. S., & Munafò, M. R. (2013). Power failure: why small sample size undermines the reliability of neuroscience. *Nature Reviews Neuroscience, 14*(5), 365-376.

Cabeza, R., Anderson, N. D., Locantore, J. K., & McIntosh, A. R. (2002). Aging gracefully: compensatory brain activity in high-performing older adults. *Neuroimage, 17*(3), 1394-1402.

Carver, A., Livesey, D., & Charles, M. (2001). Age related changes in inhibitory control as measured by stop signal task performance. *International Journal of Neuroscience, 107*(1-2), 43-61.
Cassidy, S., Mitchell, P., Chapman, P., & Ropar, D. (2015). Processing of spontaneous emotional responses in adolescents and adults with autism spectrum disorders: effect of stimulus type. *Autism Research, 8*(5), 534-544.
Chamberlain, S. R., Fineberg, N. A., Blackwell, A. D., Robbins, T. W., & Sahakian, B. J. (2006). Motor inhibition and cognitive flexibility in obsessive-compulsive disorder and trichotillomania. *American Journal of Psychiatry, 163*(7), 1282-1284.
Chambers, C. D., Bellgrove, M. A., Stokes, M. G., Henderson, T. R., Garavan, H., Robertson, I. H., . . . Mattingley, J. B. (2006). Executive "brake failure" following deactivation of human frontal lobe. *J Cogn Neurosci, 18*(3), 444-455.
Chang, A., Chen, C.-C., Li, H.-H., & Li, C.-S. R. (2014). Event-related potentials for post-error and post-conflict slowing. *PLOS ONE, 9*(6), e99909.
Chikazoe, J., Konishi, S., Asari, T., Jimura, K., & Miyashita, Y. (2007). Activation of right inferior frontal gyrus during response inhibition across response modalities. *J Cogn Neurosci, 19*(1), 69-80.
Christakou, A., Halari, R., Smith, A. B., Ifkovits, E., Brammer, M., & Rubia, K. (2009). Sex-dependent age modulation of frontostriatal and temporo-parietal activation during cognitive control. *Neuroimage, 48*(1), 223-236.
Clayson, P. E., Baldwin, S. A., & Larson, M. J. (2013). How does noise affect amplitude and latency measurement of event-related potentials (ERPs)? A methodological critique and simulation study. *Psychophysiology, 50*(2), 174-186.
Cohen, M. X. (2014). *Analyzing neural time series data: theory and practice*: MIT press.
Coles, M. G., Scheffers, M. K., & Fournier, L. (1995). Where did you go wrong? Errors, partial errors, and the nature of human information processing. *Acta psychologica, 90*(1-3), 129-144.
Corbett, B. A., & Constantine, L. J. (2006). Autism and attention deficit hyperactivity disorder: Assessing attention and response control with the integrated visual and auditory continuous performance test. *Child neuropsychology, 12*(4-5), 335-348.
Danielmeier, C., & Ullsperger, M. (2011). Post-error adjustments. *Front Psychol, 2*, 233.
de Cheveigné, A., & Simon, J. Z. (2008). Denoising based on spatial filtering. *Journal of Neuroscience Methods, 171*(2), 331-339.
De Sanctis, P., Butler, J. S., Malcolm, B. R., & Foxe, J. J. (2014). Recalibration of inhibitory control systems during walking-related dual-task interference: a mobile brain-body imaging (MOBI) study. *Neuroimage, 94*, 55-64.
De Sanctis, P., Malcolm, B. R., Mabie, P. C., Francisco, A. A., Mowrey, W. B., Joshi, S., . . . Foxe, J. J. (2020). Mobile Brain/Body Imaging of cognitive-motor impairment in multiple sclerosis: deriving EEG-based neuro-markers during a dual-task walking study. *Clinical neurophysiology, 131*(5), 1119-1128.
De Zubicaray, G., Andrew, C., Zelaya, F., Williams, S., & Dumanoir, C. (2000). Motor response suppression and the prepotent tendency to respond: a parametric fMRI study. *Neuropsychologia, 38*(9), 1280-1291.
Debener, S., Ullsperger, M., Siegel, M., Fiehler, K., Von Cramon, D. Y., & Engel, A. K. (2005). Trial-by-trial coupling of concurrent electroencephalogram and functional magnetic resonance imaging identifies the dynamics of performance monitoring. *Journal of Neuroscience, 25*(50), 11730-11737.
Delorme, A., Mullen, T., Kothe, C., Akalin Acar, Z., Bigdely-Shamlo, N., Vankov, A., & Makeig, S. (2011). EEGLAB, SIFT, NFT, BCILAB, and ERICA: new tools for advanced EEG processing. *Computational intelligence and neuroscience, 2011*.
Donkers, F. C., & Van Boxtel, G. J. (2004). The N2 in go/no-go tasks reflects conflict monitoring not response inhibition. *Brain and cognition, 56*(2), 165-176.
Dowsett, S. M., & Livesey, D. J. (2000). The development of inhibitory control in preschool children: Effects of "executive skills" training. *Developmental Psychobiology: The Journal of the International Society for Developmental Psychobiology, 36*(2), 161-174.
Drewe, E. (1975). An experimental investigation of Luria's theory on the effects of frontal lobe lesions in man. *Neuropsychologia, 13*(4), 421-429.
Durston, S., Thomas, K., Worden, M., Yang, Y., & Casey, B. (2002). The effect of preceding context on

inhibition: an event-related fMRI study. *Neuroimage, 16*(2), 449-453.
Dutilh, G., van Ravenzwaaij, D., Nieuwenhuis, S., van der Maas, H. L., Forstmann, B. U., & Wagenmakers, E.-J. (2012). How to measure post-error slowing: a confound and a simple solution. *Journal of Mathematical Psychology, 56*(3), 208-216.
Eimer, M. (1993). Effects of attention and stimulus probability on ERPs in a Go/Nogo task. *Biological psychology, 35*(2), 123-138.
Falkenstein, M., Hoormann, J., & Hohnsbein, J. (1999). ERP components in Go/Nogo tasks and their relation to inhibition. *Acta psychologica, 101*(2-3), 267-291.
Falkenstein, M., Hoormann, J., & Hohnsbein, J. (2002). Inhibition-related ERP components: variation with modality, age, and time-on-task. *Journal of Psychophysiology, 16*(3), 167.
Fallgatter, A. J., & Strik, W. K. (1999). The NoGo-anteriorization as a neurophysiological standard-index for cognitive response control. *International Journal of Psychophysiology, 32*(3), 233-238.
Ferguson, A. R., Nielson, J. L., Cragin, M. H., Bandrowski, A. E., & Martone, M. E. (2014). Big data from small data: data-sharing in the'long tail'of neuroscience. *Nat Neurosci, 17*(11), 1442-1447.
Fiehler, K., Ullsperger, M., & Von Cramon, D. Y. (2005). Electrophysiological correlates of error correction. *Psychophysiology, 42*(1), 72-82.
Filipović, S. R., Jahanshahi, M., & Rothwell, J. C. (2000). Cortical potentials related to the nogo decision. *Exp Brain Res, 132*(3), 411-415.
Floden, D., & Stuss, D. T. (2006). Inhibitory control is slowed in patients with right superior medial frontal damage. *J Cogn Neurosci, 18*(11), 1843-1849.
Folstein, J. R., & Van Petten, C. (2008). Influence of cognitive control and mismatch on the N2 component of the ERP: a review. *Psychophysiology, 45*(1), 152-170.
Fox, A., Michie, P., Wynne, C., & Maybery, M. (2000). ERP correlates of response inhibition to elemental and configural stimuli in a negative patterning task. *Clinical neurophysiology, 111*(6), 1045-1053.
Francisco, A. A., Horsthuis, D. J., Popiel, M., Foxe, J. J., & Molholm, S. (2020). Atypical response inhibition and error processing in 22q11. 2 Deletion Syndrome and Schizophrenia: Towards neuromarkers of disease progression and risk. *bioRxiv*.
Friedman, D., Simpson, G., & Hamberger, M. (1993). Age-related changes in scalp topography to novel and target stimuli. *Psychophysiology, 30*(4), 383-396.
Gajewski, P. D., & Falkenstein, M. (2013). Effects of task complexity on ERP components in Go/Nogo tasks. *International Journal of Psychophysiology, 87*(3), 273-278.
Garavan, H., Ross, T., Murphy, K., Roche, R., & Stein, E. (2002). Dissociable executive functions in the dynamic control of behavior: inhibition, error detection, and correction. *Neuroimage, 17*(4), 1820-1829.
Garavan, H., Ross, T., & Stein, E. (1999). Right hemispheric dominance of inhibitory control: an event-related functional MRI study. *Proceedings of the National Academy of Sciences, 96*(14), 8301-8306.
Gehring, W. J., & Fencsik, D. E. (2001). Functions of the medial frontal cortex in the processing of conflict and errors. *Journal of Neuroscience, 21*(23), 9430-9437.
Gehring, W. J., Goss, B., Coles, M. G., Meyer, D. E., & Donchin, E. (1993). A neural system for error detection and compensation. *Psychological Science, 4*(6), 385-390.
Godefroy, O., & Rousseaux, M. (1996). Divided and focused attention in patients with lesion of the prefrontal cortex. *Brain and cognition, 30*(2), 155-174.
Gonçalves, N. R., Whelan, R., Foxe, J. J., & Lalor, E. C. (2014). Towards obtaining spatiotemporally precise responses to continuous sensory stimuli in humans: a general linear modeling approach to EEG. *Neuroimage, 97*, 196-205.
Gorgolewski, K. J., Auer, T., Calhoun, V. D., Craddock, R. C., Das, S., Duff, E. P., . . . Halchenko, Y. O. (2016). The brain imaging data structure, a format for organizing and describing outputs of neuroimaging experiments. *Scientific data, 3*(1), 1-9.
Gramann, K., Gwin, J. T., Ferris, D. P., Oie, K., Jung, T.-P., Lin, C.-T., . . . Makeig, S. (2011). Cognition in action: imaging brain/body dynamics in mobile humans.
Grandjean, J., & Collette, F. (2011). Influence of response prepotency strength, general working memory resources, and specific working memory load on the ability to inhibit predominant responses: A comparison of young and elderly participants. *Brain and cognition, 77*(2), 237-247.

Green, D. M., & Swets, J. A. (1966). *Signal detection theory and psychophysics* (Vol. 1): Wiley New York.
Groman, S. M., James, A. S., & Jentsch, J. D. (2009). Poor response inhibition: at the nexus between substance abuse and attention deficit/hyperactivity disorder. *Neuroscience & biobehavioral reviews, 33*(5), 690-698.
Groppe, D. M., Urbach, T. P., & Kutas, M. (2011). Mass univariate analysis of event-related brain potentials/fields I: A critical tutorial review. *Psychophysiology, 48*(12), 1711-1725.
Hajcak, G., McDonald, N., & Simons, R. F. (2003). To err is autonomic: Error-related brain potentials, ANS activity, and post-error compensatory behavior. *Psychophysiology, 40*(6), 895-903.
Harmony, T., Fernández, T., Silva, J., Bernal, J., Díaz-Comas, L., Reyes, A., . . . Rodríguez, M. (1996). EEG delta activity: an indicator of attention to internal processing during performance of mental tasks. *International Journal of Psychophysiology, 24*(1-2), 161-171.
Harnishfeger, K. K., & Bjorklund, D. F. (1993). The ontogeny of inhibition mechanisms: A renewed approach to cognitive development. In *Emerging themes in cognitive development* (pp. 28-49): Springer.
Hasher, L., & Zacks, R. T. (1988). Working memory, comprehension, and aging: A review and a new view. *The psychology of learning and motivation, 22*, 193-225.
Hernández, J., Valdés, P., Biscay, R., Virues, T., Szava, S., Bosch, J., . . . Clark, I. (1994). A global scale factor in brain topography. *International Journal of Neuroscience, 76*(3-4), 267-278.
Hester, R., Foxe, J. J., Molholm, S., Shpaner, M., & Garavan, H. (2005). Neural mechanisms involved in error processing: a comparison of errors made with and without awareness. *Neuroimage, 27*(3), 602-608.
Hsieh, S., & Fang, W. (2012). Elderly adults through compensatory responses can be just as capable as young adults in inhibiting the flanker influence. *Biological psychology, 90*(2), 113-126.
Hsieh, S., Liang, Y.-C., & Tsai, Y.-C. (2012). Do age-related changes contribute to the flanker effect? *Clinical neurophysiology, 123*(5), 960-972.
Hu, S., Chao, H. H.-A., Winkler, A. D., & Li, C.-s. R. (2012). The effects of age on cerebral activations: internally versus externally driven processes. *Frontiers in aging neuroscience, 4*, 4.
Huster, R., Westerhausen, R., Pantev, C., & Konrad, C. (2010). The role of the cingulate cortex as neural generator of the N200 and P300 in a tactile response inhibition task. *Hum Brain Mapp, 31*(8), 1260-1271.
Huster, R. J., Enriquez-Geppert, S., Lavallee, C. F., Falkenstein, M., & Herrmann, C. S. (2013). Electroencephalography of response inhibition tasks: functional networks and cognitive contributions. *International Journal of Psychophysiology, 87*(3), 217-233.
Hyvärinen, A., & Oja, E. (2000). Independent component analysis: algorithms and applications. *Neural networks, 13*(4-5), 411-430.
Jackson, J. D., & Balota, D. A. (2012). Mind-wandering in younger and older adults: Converging evidence from the sustained attention to response task and reading for comprehension. *Psychology and aging, 27*(1), 106.
Jentsch, J. D., & Taylor, J. R. (1999). Impulsivity resulting from frontostriatal dysfunction in drug abuse: implications for the control of behavior by reward-related stimuli. *Psychopharmacology, 146*(4), 373-390.
Jodo, E., & Kayama, Y. (1992). Relation of a negative ERP component to response inhibition in a Go/No-go task. *Electroencephalogr Clin Neurophysiol, 82*(6), 477-482.
Johnstone, S. J., Dimoska, A., Smith, J. L., Barry, R. J., Pleffer, C. B., Chiswick, D., & Clarke, A. R. (2007). The development of stop-signal and Go/Nogo response inhibition in children aged 7–12 years: performance and event-related potential indices. *International Journal of Psychophysiology, 63*(1), 25-38.
Jonkman, L., Sniedt, F., & Kemner, C. (2007). Source localization of the Nogo-N2: a developmental study. *Clinical neurophysiology, 118*(5), 1069-1077.
Jonkman, L. M. (2006). The development of preparation, conflict monitoring and inhibition from early childhood to young adulthood; a Go/Nogo ERP study. *Brain research, 1097*(1), 181-193.
Katz, R., De Sanctis, P., Mahoney, J. R., Sehatpour, P., Murphy, C. F., Gomez-Ramirez, M., . . . Foxe, J. J. (2010). Cognitive control in late-life depression: response inhibition deficits and dysfunction of the anterior cingulate cortex. *The American Journal of Geriatric Psychiatry, 18*(11), 1017-

1025.
Kawashima, R., Satoh, K., Itoh, H., Ono, S., Furumoto, S., Gotoh, R., . . . Takahashi, K. (1996). Functional anatomy of GO/NO-GO discrimination and response selection—a PET study in man. *Brain research, 728*(1), 79-89.
Keating, D. P., & Bobbitt, B. L. (1978). Individual and developmental differences in cognitive-processing components of mental ability. *Child Development*, 155-167.
Kerns, J. G., Cohen, J. D., MacDonald, A. W., Cho, R. Y., Stenger, V. A., & Carter, C. S. (2004). Anterior cingulate conflict monitoring and adjustments in control. *Science, 303*(5660), 1023-1026.
King, J. A., Korb, F. M., von Cramon, D. Y., & Ullsperger, M. (2010). Post-error behavioral adjustments are facilitated by activation and suppression of task-relevant and task-irrelevant information processing. *Journal of Neuroscience, 30*(38), 12759-12769.
Konishi, S., Kawazu, M., Uchida, I., Kikyo, H., Asakura, I., & Miyashita, Y. (1999). Contribution of working memory to transient activation in human inferior prefrontal cortex during performance of the Wisconsin Card Sorting Test. *Cerebral Cortex, 9*(7), 745-753.
Konishi, S., Nakajima, K., Uchida, I., Sekihara, K., & Miyashita, Y. (1998). No-go dominant brain activity in human inferior prefrontal cortex revealed by functional magnetic resonance imaging. *European Journal of Neuroscience, 10*(3), 1209-1213.
Krakowski, M. I., De Sanctis, P., Foxe, J. J., Hoptman, M. J., Nolan, K., Kamiel, S., & Czobor, P. (2016). Disturbances in response inhibition and emotional processing as potential pathways to violence in schizophrenia: a high-density event-related potential study. *Schizophrenia bulletin, 42*(4), 963-974.
Kropotov, J., Ponomarev, V., Tereshchenko, E. P., Müller, A., & Jäncke, L. (2016). Effect of aging on ERP components of cognitive control. *Frontiers in aging neuroscience, 8*, 69.
Kropotov, J. D., Ponomarev, V. A., Hollup, S., & Mueller, A. (2011). Dissociating action inhibition, conflict monitoring and sensory mismatch into independent components of event related potentials in GO/NOGO task. *Neuroimage, 57*(2), 565-575.
Krueger, C., & Tian, L. (2004). A comparison of the general linear mixed model and repeated measures ANOVA using a dataset with multiple missing data points. *Biological research for nursing, 6*(2), 151-157.
Kuiper, M. W., Verhoeven, E. W., & Geurts, H. M. (2016). The role of interstimulus interval and "stimulus-type" in prepotent response inhibition abilities in people with ASD: A quantitative and qualitative review. *Autism Research, 9*(11), 1124-1141.
Laming, D. (1979). Choice reaction performance following an error. *Acta psychologica, 43*(3), 199-224.
Lang, P. J., Bradley, M. M., & Cuthbert, B. N. (1997). International affective picture system (IAPS): Technical manual and affective ratings. *NIMH Center for the Study of Emotion and Attention, 1*, 39-58.
Langenecker, S. A., & Nielson, K. A. (2003). Frontal recruitment during response inhibition in older adults replicated with fMRI. *Neuroimage, 20*(2), 1384-1392.
Leavitt, V. M., Molholm, S., Ritter, W., Shpaner, M., & Foxe, J. J. (2007). Auditory processing in schizophrenia during the middle latency period (10-50 ms): high-density electrical mapping and source analysis reveal subcortical antecedents to early cortical deficits. *Journal of psychiatry & neuroscience*.
Lee, P. S., Yerys, B. E., Della Rosa, A., Foss-Feig, J., Barnes, K. A., James, J. D., . . . Kenworthy, L. E. (2009). Functional connectivity of the inferior frontal cortex changes with age in children with autism spectrum disorders: a fcMRI study of response inhibition. *Cerebral Cortex, 19*(8), 1787-1794.
Leuchter, A. F., Cook, I. A., Newton, T. F., Dunkin, J., Walter, D. O., Rosenberg-Thompson, S., . . . Weiner, H. (1993). Regional differences in brain electrical activity in dementia: use of spectral power and spectral ratio measures. *Electroencephalogr Clin Neurophysiol, 87*(6), 385-393.
Liddle, P. F., Kiehl, K. A., & Smith, A. M. (2001). Event-related fMRI study of response inhibition. *Hum Brain Mapp, 12*(2), 100-109.
Liston, C., Watts, R., Tottenham, N., Davidson, M. C., Niogi, S., Ulug, A. M., & Casey, B. (2006). Frontostriatal microstructure modulates efficient recruitment of cognitive control. *Cerebral Cortex, 16*(4), 553-560.
Loree, A. M., Lundahl, L. H., & Ledgerwood, D. M. (2015). Impulsivity as a predictor of treatment

outcome in substance use disorders: Review and synthesis. *Drug and alcohol review, 34*(2), 119-134.
Lucci, G., Berchicci, M., Spinelli, D., Taddei, F., & Di Russo, F. (2013). The effects of aging on conflict detection. *PLOS ONE, 8*(2), e56566.
Luck, S. J., & Gaspelin, N. (2017). How to get statistically significant effects in any ERP experiment (and why you shouldn't). *Psychophysiology, 54*(1), 146-157.
Luke, S. G. (2017). Evaluating significance in linear mixed-effects models in R. *Behavior research methods, 49*(4), 1494-1502.
Lustig, C., Hasher, L., & Zacks, R. T. (2007). Inhibitory deficit theory: Recent developments in a" new view".
Macmillan, N. A., & Creelman, C. D. (2004). *Detection theory: A user's guide*: Psychology press.
Makeig, S., Gramann, K., Jung, T.-P., Sejnowski, T. J., & Poizner, H. (2009). Linking brain, mind and behavior. *International Journal of Psychophysiology, 73*(2), 95-100.
Malcolm, B. R., Foxe, J. J., Butler, J. S., & De Sanctis, P. (2015). The aging brain shows less flexible reallocation of cognitive resources during dual-task walking: a mobile brain/body imaging (MoBI) study. *Neuroimage, 117*, 230-242.
Malcolm, B. R., Foxe, J. J., Butler, J. S., Mowrey, W. B., Molholm, S., & De Sanctis, P. (2019). Long-term test-retest reliability of event-related potential (ERP) recordings during treadmill walking using the mobile brain/body imaging (MoBI) approach. *Brain research, 1716*, 62-69.
Maylor, E. A., Birak, K. S., & Schlaghecken, F. (2011). Inhibitory motor control in old age: evidence for de-automatization? *Front Psychol, 2*, 132.
McDowd, J. M., Oseas-Kreger, D. M., & Filion, D. L. (1995). Inhibitory processes in cognition and aging. *Interference and inhibition in cognition*, 363-400.
McEvoy, L. K., Pellouchoud, E., Smith, M. E., & Gevins, A. (2001). Neurophysiological signals of working memory in normal aging. *Cognitive Brain Research, 11*(3), 363-376.
Metin, B., Roeyers, H., Wiersema, J. R., van der Meere, J., & Sonuga-Barke, E. (2012). A meta-analytic study of event rate effects on Go/No-Go performance in attention-deficit/hyperactivity disorder. *Biological psychiatry, 72*(12), 990-996.
Milham, M. P. (2012). Open neuroscience solutions for the connectome-wide association era. *Neuron, 73*(2), 214-218.
Morey, R. D., Rouder, J. N., & Jamil, T. (2015). BayesFactor: Computation of Bayes factors for common designs. R package version 0.9. 12-2. In.
Morie, K. P., De Sanctis, P., Garavan, H., & Foxe, J. J. (2014). Executive dysfunction and reward dysregulation: a high-density electrical mapping study in cocaine abusers. *Neuropharmacology, 85*, 397-407.
Morie, K. P., Garavan, H., Bell, R. P., De Sanctis, P., Krakowski, M. I., & Foxe, J. J. (2014). Intact inhibitory control processes in abstinent drug abusers (II): a high-density electrical mapping study in former cocaine and heroin addicts. *Neuropharmacology, 82*, 151-160.
Mostofsky, S. H., Schafer, J. G., Abrams, M. T., Goldberg, M. C., Flower, A. A., Boyce, A., . . . Denckla, M. B. (2003). fMRI evidence that the neural basis of response inhibition is task-dependent. *Cognitive Brain Research, 17*(2), 419-430.
Müller, V., Gruber, W., Klimesch, W., & Lindenberger, U. (2009). Lifespan differences in cortical dynamics of auditory perception. *Developmental science, 12*(6), 839-853.
Murray, M. M., Wylie, G. R., Higgins, B. A., Javitt, D. C., Schroeder, C. E., & Foxe, J. J. (2002). The spatiotemporal dynamics of illusory contour processing: combined high-density electrical mapping, source analysis, and functional magnetic resonance imaging. *Journal of Neuroscience, 22*(12), 5055-5073.
Nielson, K. A., Langenecker, S. A., & Garavan, H. (2002). Differences in the functional neuroanatomy of inhibitory control across the adult life span. *Psychology and aging, 17*(1), 56.
Nieuwenhuis, S., Aston-Jones, G., & Cohen, J. D. (2005). Decision making, the P3, and the locus coeruleus--norepinephrine system. *Psychol Bull, 131*(4), 510.
Nieuwenhuis, S., Ridderinkhof, K. R., Blom, J., Band, G. P., & Kok, A. (2001). Error-related brain potentials are differentially related to awareness of response errors: Evidence from an antisaccade task. *Psychophysiology, 38*(5), 752-760.
Nieuwenhuis, S., Yeung, N., Van Den Wildenberg, W., & Ridderinkhof, K. R. (2003).

Electrophysiological correlates of anterior cingulate function in a go/no-go task: effects of response conflict and trial type frequency. *Cognitive, affective, & behavioral neuroscience, 3*(1), 17-26.
Notebaert, W., Houtman, F., Van Opstal, F., Gevers, W., Fias, W., & Verguts, T. (2009). Post-error slowing: an orienting account. *Cognition, 111*(2), 275-279.
núñez Castellar, E., Kühn, S., Fias, W., & Notebaert, W. (2010). Outcome expectancy and not accuracy determines posterror slowing: ERP support. *Cognitive, affective, & behavioral neuroscience, 10*(2), 270-278.
Nunez, P. L., Srinivasan, R., Westdorp, A. F., Wijesinghe, R. S., Tucker, D. M., Silberstein, R. B., & Cadusch, P. J. (1997). EEG coherency: I: statistics, reference electrode, volume conduction, Laplacians, cortical imaging, and interpretation at multiple scales. *Electroencephalogr Clin Neurophysiol, 103*(5), 499-515.
Nuwer, M. R. (1988). Quantitative EEG: I. Techniques and problems of frequency analysis and topographic mapping. *Journal of clinical neurophysiology: official publication of the American Electroencephalographic Society, 5*(1), 1-43.
Oerlemans, A. M., Droste, K., van Steijn, D. J., de Sonneville, L. M., Buitelaar, J. K., & Rommelse, N. N. (2013). Co-segregation of social cognition, executive function and local processing style in children with ASD, their siblings and normal controls. *Journal of autism and developmental disorders, 43*(12), 2764-2778.
Ojeda, A., Bigdely-Shamlo, N., & Makeig, S. (2014). MoBILAB: an open source toolbox for analysis and visualization of mobile brain/body imaging data. *Frontiers in human neuroscience, 8*, 121.
Oostenveld, Fries, P., Maris, E., & Schoffelen, J. M. (2011). FieldTrip: Open source software for advanced analysis of MEG, EEG, and invasive electrophysiological data. *Comput Intell Neurosci, 2011*, 156869. doi:10.1155/2011/156869
Oostenveld, R., & Maris, E. (2007). Nonparametric statistical testing of EEG-and MEG-data. Retrieved from https://www.scienceopen.com/document?id=327268fe-fbce-4b64-99c0-912f7ccc419e
https://www.sciencedirect.com/science/article/pii/S0165027007001707
Orr, C., & Hester, R. (2012). Error-related anterior cingulate cortex activity and the prediction of conscious error awareness. *Frontiers in human neuroscience, 6*, 177.
Pailing, P. E., & Segalowitz, S. J. (2004). The error-related negativity as a state and trait measure: Motivation, personality, and ERPs in response to errors. *Psychophysiology, 41*(1), 84-95.
Pascual-Marqui, R. D., Michel, C. M., & Lehmann, D. (1994). Low resolution electromagnetic tomography: a new method for localizing electrical activity in the brain. *International Journal of Psychophysiology, 18*(1), 49-65.
Passler, M. A., Isaac, W., & Hynd, G. W. (1985). Neuropsychological development of behavior attributed to frontal lobe functioning in children. *Developmental neuropsychology, 1*(4), 349-370.
Patelaki, E., Foxe, J. J., Mazurek, K. A., & Freedman, E. G. (2022). Young adults who improve performance during dual-task walking show more flexible reallocation of cognitive resources: A Mobile Brain-Body Imaging (MoBI) study. *bioRxiv*.
Pernet, C. R., Wilcox, R. R., & Rousselet, G. A. (2013). Robust correlation analyses: false positive and power validation using a new open source matlab toolbox. *Front Psychol, 3*, 606.
Perri, R. L., Berchicci, M., Lucci, G., Spinelli, D., & Di Russo, F. (2016). How the brain prevents a second error in a perceptual decision-making task. *Scientific Reports, 6*, 32058.
Pfefferbaum, A., & Ford, J. M. (1988). ERPs to stimuli requiring response production and inhibition: effects of age, probability and visual noise. *Electroencephalography and Clinical Neurophysiology/Evoked Potentials Section, 71*(1), 55-63.
Pfefferbaum, A., Ford, J. M., Weller, B. J., & Kopell, B. S. (1985). ERPs to response production and inhibition. *Electroencephalogr Clin Neurophysiol, 60*(5), 423-434.
Philip, R. C., Whalley, H. C., Stanfield, A. C., Sprengelmeyer, R., Santos, I. M., Young, A. W., . . . Lawrie, S. (2010). Deficits in facial, body movement and vocal emotional processing in autism spectrum disorders. *Psychological medicine, 40*(11), 1919-1929.
Phillips, L. H., & Andrés, P. (2010). The cognitive neuroscience of aging: new findings on compensation and connectivity. *Cortex, 4*(46), 421-424.
Picton, T. W., Stuss, D. T., Alexander, M. P., Shallice, T., Binns, M. A., & Gillingham, S. (2007). Effects of focal frontal lesions on response inhibition. *Cerebral Cortex, 17*(4), 826-838.

Pion-Tonachini, L., Kreutz-Delgado, K., & Makeig, S. (2019). The ICLabel dataset of electroencephalographic (EEG) independent component (IC) features. *Data in brief, 25*, 104101.
Pion-Tonachini, L., Kreutz-Delgado, K., & Makeig, S. (2019). ICLabel: An automated electroencephalographic independent component classifier, dataset, and website. *Neuroimage, 198*, 181-197.
Pires, L., Leitão, J., Guerrini, C., & Simões, M. R. (2014). Event-related brain potentials in the study of inhibition: cognitive control, source localization and age-related modulations. *Neuropsychology review, 24*(4), 461-490.
Poldrack, R. A. (2012). The future of fMRI in cognitive neuroscience. *Neuroimage, 62*(2), 1216-1220.
Poldrack, R. A., & Gorgolewski, K. J. (2014). Making big data open: data sharing in neuroimaging. *Nat Neurosci, 17*(11), 1510-1517.
Rabbitt, P. (1966). Errors and error correction in choice-response tasks. *Journal of experimental psychology, 71*(2), 264.
Rabbitt, P., & Rodgers, B. (1977). What does a man do after he makes an error? An analysis of response programming. *Quarterly Journal of Experimental Psychology, 29*(4), 727-743.
Randall, W. M., & Smith, J. L. (2011). Conflict and inhibition in the cued-Go/NoGo task. *Clinical neurophysiology, 122*(12), 2400-2407.
Rey-Mermet, A., & Gade, M. (2018). Inhibition in aging: What is preserved? What declines? A meta-analysis. *Psychonomic Bulletin & Review, 25*(5), 1695-1716.
Riccio, C. A., Reynolds, C. R., Lowe, P., & Moore, J. J. (2002). The continuous performance test: a window on the neural substrates for attention? *Archives of clinical neuropsychology, 17*(3), 235-272.
Ridderinkhof, K. R., Van Den Wildenberg, W. P., Segalowitz, S. J., & Carter, C. S. (2004). Neurocognitive mechanisms of cognitive control: the role of prefrontal cortex in action selection, response inhibition, performance monitoring, and reward-based learning. *Brain and cognition, 56*(2), 129-140.
Ridderinkhof, R. K. (2002). Micro-and macro-adjustments of task set: activation and suppression in conflict tasks. *Psychol Res, 66*(4), 312-323.
Rietdijk, W. J., Franken, I. H., & Thurik, A. R. (2014). Internal consistency of event-related potentials associated with cognitive control: N2/P3 and ERN/Pe. *PLOS ONE, 9*(7), e102672.
Roche, R. A., Dockree, P. M., Garavan, H., Foxe, J. J., Robertson, I. H., & O'Mara, S. M. (2004). EEG alpha power changes reflect response inhibition deficits after traumatic brain injury (TBI) in humans. *Neurosci Lett, 362*(1), 1-5.
Rodríguez-Fornells, A., Kurzbuch, A. R., & Münte, T. F. (2002). Time course of error detection and correction in humans: neurophysiological evidence. *Journal of Neuroscience, 22*(22), 9990-9996.
Rouder, J. N., Morey, R. D., Speckman, P. L., & Province, J. M. (2012). Default Bayes factors for ANOVA designs. *Journal of Mathematical Psychology, 56*(5), 356-374.
Rouder, J. N., Speckman, P. L., Sun, D., Morey, R. D., & Iverson, G. (2009). Bayesian t tests for accepting and rejecting the null hypothesis. *Psychonomic Bulletin & Review, 16*(2), 225-237.
Rousselet, G. A. (2012). Does filtering preclude us from studying ERP time-courses? *Front Psychol, 3*, 131.
Rubia, K., Russell, T., Overmeyer, S., Brammer, M. J., Bullmore, E. T., Sharma, T., . . . Andrew, C. M. (2001). Mapping motor inhibition: conjunctive brain activations across different versions of go/no-go and stop tasks. *Neuroimage, 13*(2), 250-261.
Ruchsow, M., Groen, G., Kiefer, M., Hermle, L., Spitzer, M., & Falkenstein, M. (2008). Impulsiveness and ERP components in a Go/Nogo task. *Journal of Neural Transmission, 115*(6), 909-915.
Rush, B. K., Barch, D. M., & Braver, T. S. (2006). Accounting for cognitive aging: context processing, inhibition or processing speed? *Aging, Neuropsychology, and Cognition, 13*(3-4), 588-610.
Saint-Amour, D., De Sanctis, P., Molholm, S., Ritter, W., & Foxe, J. J. (2007). Seeing voices: High-density electrical mapping and source-analysis of the multisensory mismatch negativity evoked during the McGurk illusion. *Neuropsychologia, 45*(3), 587-597. doi:10.1016/j.neuropsychologia.2006.03.036
Salisbury, D. F., Griggs, C. B., Shenton, M. E., & McCarley, R. W. (2004). The NoGo P300 'anteriorization'effect and response inhibition. *Clinical neurophysiology, 115*(7), 1550-1558.
Schachar, R., & Logan, G. D. (1990). Impulsivity and inhibitory control in normal development and

childhood psychopathology. *Developmental psychology, 26*(5), 710.
Schmiedt-Fehr, C., Mathes, B., Kedilaya, S., Krauss, J., & Basar-Eroglu, C. (2016). Aging differentially affects alpha and beta sensorimotor rhythms in a go/nogo task. *Clinical neurophysiology, 127*(10), 3234-3242.
Schönbrodt, F. D., Wagenmakers, E.-J., Zehetleitner, M., & Perugini, M. (2017). Sequential hypothesis testing with Bayes factors: Efficiently testing mean differences. *Psychological methods, 22*(2), 322.
Simmonds, D. J., Pekar, J. J., & Mostofsky, S. H. (2008). Meta-analysis of Go/No-go tasks demonstrating that fMRI activation associated with response inhibition is task-dependent. *Neuropsychologia, 46*(1), 224-232.
Smallwood, J., Davies, J. B., Heim, D., Finnigan, F., Sudberry, M., O'Connor, R., & Obonsawin, M. (2004). Subjective experience and the attentional lapse: Task engagement and disengagement during sustained attention. *Consciousness and cognition, 13*(4), 657-690.
Smith, J. L., Johnstone, S. J., & Barry, R. J. (2007). Response priming in the Go/NoGo task: the N2 reflects neither inhibition nor conflict. *Clinical neurophysiology, 118*(2), 343-355.
Soshi, T., Ando, K., Noda, T., Nakazawa, K., Tsumura, H., & Okada, T. (2015). Post-error action control is neurobehaviorally modulated under conditions of constant speeded response. *Frontiers in human neuroscience, 8*, 1072.
Stam, C. J., Nolte, G., & Daffertshofer, A. (2007). Phase lag index: assessment of functional connectivity from multi channel EEG and MEG with diminished bias from common sources. *Hum Brain Mapp, 28*(11), 1178-1193.
Strik, W., Fallgatter, A., Brandeis, D., & Pascual-Marqui, R. (1998). Three-dimensional tomography of event-related potentials during response inhibition: evidence for phasic frontal lobe activation. *Electroencephalography and Clinical Neurophysiology/Evoked Potentials Section, 108*(4), 406-413.
Tamm, L., Menon, V., & Reiss, A. L. (2002). Maturation of brain function associated with response inhibition. *Journal of the American Academy of Child & Adolescent Psychiatry, 41*(10), 1231-1238.
Tanner, D., Morgan-Short, K., & Luck, S. J. (2015). How inappropriate high-pass filters can produce artifactual effects and incorrect conclusions in ERP studies of language and cognition. *Psychophysiology, 52*(8), 997-1009.
Taylor, S. F., Stern, E. R., & Gehring, W. J. (2007). Neural systems for error monitoring: recent findings and theoretical perspectives. *The Neuroscientist, 13*(2), 160-172.
Ullsperger, M., & Falkenstein, M. (2004). Errors, conflicts, and the brain. Current opinions on performance monitoring. *Leipzig: MPI of Cognitive Neuroscience*.
Ullsperger, M., Fischer, A. G., Nigbur, R., & Endrass, T. (2014). Neural mechanisms and temporal dynamics of performance monitoring. *Trends Cogn Sci, 18*(5), 259-267.
Vallesi, A. (2011). Targets and non-targets in the aging brain: a go/nogo event-related potential study. *Neurosci Lett, 487*(3), 313-317.
Vallesi, A., & Stuss, D. T. (2010). Excessive sub-threshold motor preparation for non-target stimuli in normal aging. *Neuroimage, 50*(3), 1251-1257.
Vallesi, A., Stuss, D. T., McIntosh, A. R., & Picton, T. W. (2009). Age-related differences in processing irrelevant information: evidence from event-related potentials. *Neuropsychologia, 47*(2), 577-586.
van Boxtel, G. J., van der Molen, M. W., Jennings, J. R., & Brunia, C. H. (2001). A psychophysiological analysis of inhibitory motor control in the stop-signal paradigm. *Biological psychology, 58*(3), 229-262.
Van der Lubbe, R. H., & Verleger, R. (2002). Aging and the Simon task. *Psychophysiology, 39*(1), 100-110.
Van der Oord, S., Geurts, H., Prins, P., Emmelkamp, P., & Oosterlaan, J. (2012). Prepotent response inhibition predicts treatment outcome in attention deficit/hyperactivity disorder. *Child neuropsychology, 18*(1), 50-61.
Verbruggen, F., Aron, A. R., Band, G. P., Beste, C., Bissett, P. G., Brockett, A. T., . . . Colonius, H. (2019). A consensus guide to capturing the ability to inhibit actions and impulsive behaviors in the stop-signal task. *eLife, 8*, e46323.

Verbruggen, F., & Logan, G. D. (2008). Automatic and controlled response inhibition: associative learning in the go/no-go and stop-signal paradigms. *Journal of Experimental Psychology: General, 137*(4), 649.

Vinck, M., Oostenveld, R., Van Wingerden, M., Battaglia, F., & Pennartz, C. M. (2011). An improved index of phase-synchronization for electrophysiological data in the presence of volume-conduction, noise and sample-size bias. *Neuroimage, 55*(4), 1548-1565.

Viola, F. C., Debener, S., Thorne, J., & Schneider, T. R. (2010). Using ICA for the analysis of multi-channel EEG data. *Simultaneous EEG and fMRI: Recording, Analysis, and Application: Recording, Analysis, and Application*, 121-133.

Vuillier, L., Bryce, D., Szücs, D., & Whitebread, D. (2016). The maturation of interference suppression and response inhibition: ERP analysis of a cued Go/Nogo task. *PLOS ONE, 11*(11), e0165697.

Wagenmakers, E.-J., Wetzels, R., Borsboom, D., & Van Der Maas, H. L. (2011). Why psychologists must change the way they analyze their data: the case of psi: comment on Bem (2011).

Wager, T. D., Sylvester, C.-Y. C., Lacey, S. C., Nee, D. E., Franklin, M., & Jonides, J. (2005). Common and unique components of response inhibition revealed by fMRI. *Neuroimage, 27*(2), 323-340.

Wainwright, P. E., Leatherdale, S. T., & Dubin, J. A. (2007). Advantages of mixed effects models over traditional ANOVA models in developmental studies: a worked example in a mouse model of fetal alcohol syndrome. *Developmental Psychobiology: The Journal of the International Society for Developmental Psychobiology, 49*(7), 664-674.

Wakim, K.-M., Freedman, E. G., Molloy, C. J., Vieyto, N., Cao, Z., & Foxe, J. J. (2021). Assessing combinatorial effects of HIV infection and former cocaine dependence on cognitive control processes: A high-density electrical mapping study of response inhibition. *Neuropharmacology*, 108636.

Watanabe, J., Sugiura, M., Sato, K., Sato, Y., Maeda, Y., Matsue, Y., . . . Kawashima, R. (2002). The human prefrontal and parietal association cortices are involved in NO-GO performances: an event-related fMRI study. *Neuroimage, 17*(3), 1207-1216.

Wessel, J. R. (2012). Error awareness and the error-related negativity: evaluating the first decade of evidence. *Frontiers in human neuroscience, 6*, 88.

Wessel, J. R. (2018). Prepotent motor activity and inhibitory control demands in different variants of the go/no-go paradigm. *Psychophysiology, 55*(3), e12871.

Wessel, J. R., & Aron, A. R. (2015). It's not too late: The onset of the frontocentral P 3 indexes successful response inhibition in the stop-signal paradigm. *Psychophysiology, 52*(4), 472-480.

Wessel, J. R., & Ullsperger, M. (2011). Selection of independent components representing event-related brain potentials: a data-driven approach for greater objectivity. *Neuroimage, 54*(3), 2105-2115.

West, R., & Alain, C. (2000). Age-related decline in inhibitory control contributes to the increased Stroop effect observed in older adults. *Psychophysiology, 37*(2), 179-189.

West, R., & Travers, S. (2008). Tracking the temporal dynamics of updating cognitive control: An examination of error processing. *Cerebral Cortex, 18*(5), 1112-1124.

Williams, B. R., Ponesse, J. S., Schachar, R. J., Logan, G. D., & Tannock, R. (1999). Development of inhibitory control across the life span. *Developmental psychology, 35*(1), 205.

Winkler, I., Debener, S., Müller, K.-R., & Tangermann, M. (2015). *On the influence of high-pass filtering on ICA-based artifact reduction in EEG-ERP*. Paper presented at the 2015 37th Annual International Conference of the IEEE Engineering in Medicine and Biology Society (EMBC).

Yeung, N., Botvinick, M. M., & Cohen, J. D. (2004). The neural basis of error detection: conflict monitoring and the error-related negativity. *Psychol Rev, 111*(4), 931.

Zamorano, F., Billeke, P., Hurtado, J. M., López, V., Carrasco, X., Ossandón, T., & Aboitiz, F. (2014). Temporal constraints of behavioral inhibition: relevance of inter-stimulus interval in a Go-Nogo task. *PLOS ONE, 9*(1), e87232.

Zelazo, P. D., Frye, D., & Rapus, T. (1996). An age-related dissociation between knowing rules and using them. *Cognitive development, 11*(1), 37-63.

Zheng, D., Oka, T., Bokura, H., & Yamaguchi, S. (2008). The key locus of common response inhibition network for no-go and stop signals. *J Cogn Neurosci, 20*(8), 1434-1442.